A cerebellar population coding model for sensorimotor learning

Tianhe Wang*, Richard B. Ivry

Department of Psychology and Helen Wills Neuroscience Institute, University of California, Berkeley, California

Corresponding authors (*):

Tianhe Wang (tianhewang@berkeley.edu)

Summary

The cerebellum plays a critical role in sensorimotor learning, using error information to keep the sensorimotor system well-calibrated. Here we present a population-coding model of how the cerebellum compensates for motor errors. The model consists of a two-layer network, with one layer corresponding to the cerebellar cortex and the other to the deep cerebellar nuclei. Units within each layer are tuned to two features: the direction of the movement and the direction of the error. To evaluate the model, we conducted a series of behavioral experiments using a wide range of perturbation schedules. The model successfully accounts for interference from prior learning, the effects of error uncertainties, and learning in response to perturbations that vary across different time scales. Importantly, the model does not require any modulation of the parameters or context-dependent processes during adaptation. Our results provide a novel framework to understand how context and environmental uncertainty modulate learning.

Keywords

Sensorimotor Learning, Cerebellum, Context, Environmental Variability, Population Coding

Introduction

Humans are incredibly flexible in how we adapt our motor behavior across variable environments. We readily compensate for the added weight of a heavy winter coat when reaching for an object or adjust the force required as we sip on our morning coffee. The cerebellum is recognized as playing a key role in this adaptation process[1,2], utilizing errors as teaching signals to improve subsequent, similar movements[3,4]. This form of learning operates implicitly, automatically recalibrating the sensorimotor system without the need for awareness or drawing on cognitive resources[5–7]. The current paper aims to understand how this recalibration process is modified by context and environmental uncertainty.

Previous research has suggested that cerebellum-dependent learning is cognitively impenetrable, responding to error in a rigid manner even when the correction fails to improve task performance[5,8–11]. Moreover, unlike many learning processes, adaptation is not sensitive to the statistical properties of the perturbations[12,13]. However, this view of a rigid, inflexible system has been challenged by recent evidence showing that implicit adaptation is modulated by experience[14]. For instance, when participants are exposed to a previously experienced perturbation, the rate of relearning is slower than had been originally observed[15]. Not only does this result suggest a degree of flexibility in adaptation, but this context effect is opposite what is typically observed in studies of relearning: Across a broad range of task domains, relearning is typically faster, a phenomenon known as savings[16–18].

The rigidity and atypical effect of experience point to the need for considering the unique properties of the cerebellum in understanding how adaptation is modulated by experience and environmental variability. To this end, we incorporated two core observations from cerebellar physiology to develop a general model of cerebellar-dependent learning. First, recent studies of oculomotor control have revealed a fundamental tuning property of Purkinje cells, the primary integrative unit in the cerebellar

cortex: These cells are not only tuned to movement direction but also to the direction of error relative to that movement[19–21] (Fig 1b). Second, learning is not confined to the cerebellar cortex; it also takes place in the deep cerebellar nuclei[22–25]. By positing an architecture in which units that share similar tuning profiles are linked across these two layers, we develop a cerebellar population coding (CPC) model.

To validate our model, we conducted a series of behavioral experiments employing various perturbation schedules. Specifically, we examined the effect of past experience, error uncertainty, error size, and variation in temporal dynamics in evaluating our model. Where relevant, we consider several alternative models that have been proposed to elucidate how context and environmental uncertainty modulate sensorimotor learning[26–28]. Our population-coding model provides the best fit in all the behavioral tests, even without positing context-dependent learning or having the capability to modulate learning parameters. As such, these results point to a parsimonious model of how the cerebellum supports sensorimotor adaptation across a broad range of contexts.

Results

Cerebellar Population Coding (CPC) Model

The basic principles of cerebellar-dependent error-based learning are articulated in the classic Marr-Albus model[2,29]. Purkinje cells (PC) in the cerebellar cortex receive two types of input (Fig 1a). One source originates in the pontine nuclei. This pathway is hypothesized to provides contextual information, including an efference copy of the motor command. PCs operate as an internal model, utilizing the input to predict the consequences of the motor command[30,31]. The second source originates in the inferior olive with activation of the climbing fibers indicating a mismatch between the predicted and expected sensory feedback, a teaching signal that is used to update the internal model.

Here we extend the model to provide a general explanation of how learning is modulated by contextual variability. A foundational idea for our model is inspired by a recent work showing how PCs in the oculomotor cerebellar cortex are simultaneously tuned to both movement direction and the direction of a visual error that arises during that movement[19–21] (Fig 1b, c). Tuning in terms of movement direction is reflected in the simple spike activity of the Purkinje cells and tuning in terms of movement error is reflected in the complex spike activity of these cells. The latter one induces long-term depression (LTD) of parallel fiber-PC (PF-PC) synapses, reducing the future efficacy of similar input on PC activity (Fig 1d). Importantly, because the two tuning profiles are in opposite directions[19–21], error-related activation will result in a change in the output, thus reducing the error.

A second prominent feature of our model is that plasticity occurs within the cerebellar cortex and deep cerebellar nuclei (DCN)[22,32]. Lesion studies of eyeblink conditioning provide one line of evidence indicating that some aspect of consolidated learning is centered in the DCN. Ablation of the cerebellar cortex can completely block *de novo* cerebellar-dependent learning[23,33]. However, once the learned behavior is established, it can persist after lesions to the cerebellar cortex even though the kinematics are disrupted[34,35]. This dissociation can be explained by the dual-effect of pontine projections to the cerebellum[36]: a polysynaptic projection through the granule layer to PC, and a direct excitatory projection of the mossy fibers to the DCN. Importantly, we assume that PC and DCN neurons are connected such that they share the same tuning direction for movement[37], and that learning in the DCN is gated by learning at the cerebellar cortex (Fig 1a). Specifically, LTD at parallel fiber-PC (PF-PC) synapses will reduce inhibitory PC input to the DCN, resulting in long term potentiation (LTP) at the mossy fiber-DCN synapses (Fig 1e).

In summary, an error signal will decrease the efficacy of parallel fiber input to PCs and increase the efficacy of mossy fiber input to the DCN (Fig 1d, e). Correspondingly, the net output of the cerebellum will provide a signal of the required change in movement direction to correct for the error (Fig 1f).

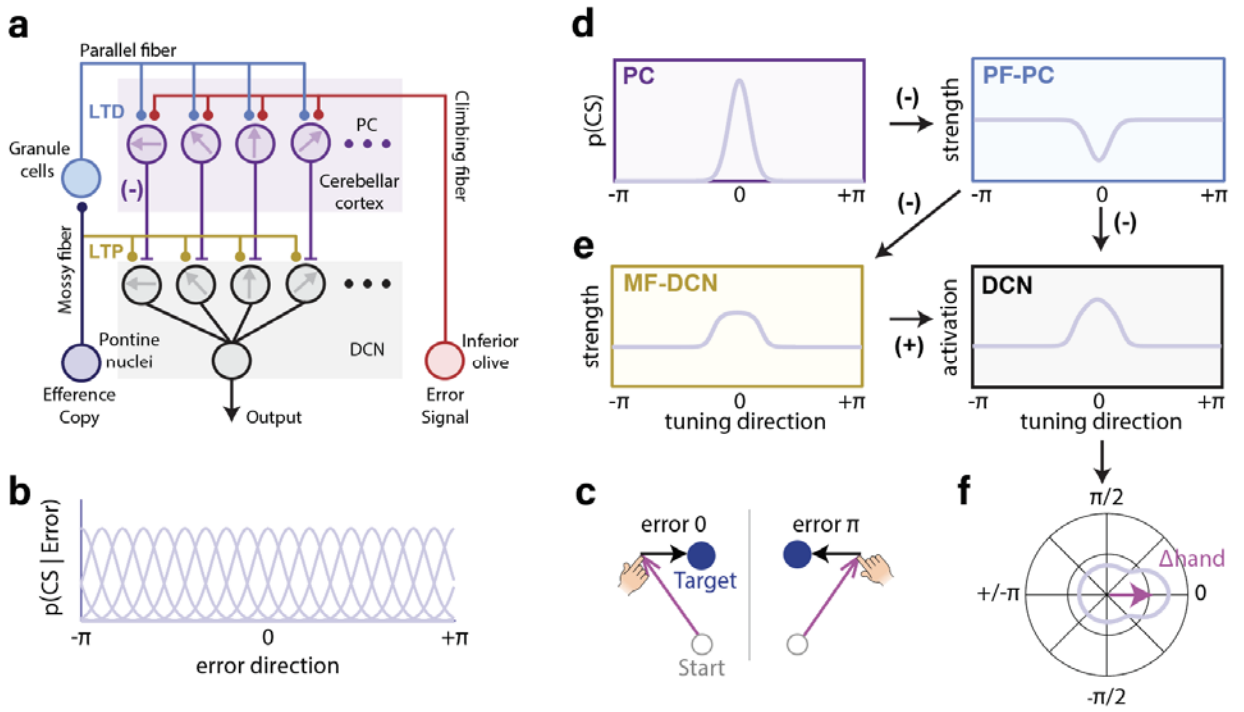

Fig. 1 Illustration of the CPC model. a) Structure of the cerebellar circuit incorporated in the CPC model. **b)** Each Gaussian-shaped curve represents the tuning function of a single Purkinje cell (PC) based on that cell's preferred error direction. For the simulations, we used 1000 units with preferred directions that covered 0-π in a uniform manner. **c)** Illustration of visual errors, with the direction of the error specified in polar coordinates. **d-e)** Model-generated adaptation in the cerebellar cortex (d) and deep cerebellar nuclei (DCN) (e). After experiencing an error in 0 direction, PC's with a preferred direction close to 0 will have high probability of generating a complex spike (CS) (d, left) which will result in long-term depression (LTD) for active synapses from granule cell inputs to that PC (d, right). During the preparation of the next movement, the strength of the input from the parallel fibers (PF) will decrease due LTD, attenuating the SS activity of the PC. Attenuation of PC output will result in long-term potentiation (LTP) at the mossy fiber (MF) input synapse to DCN (e, left). DCN activation is determined by the excitatory input from the MF and the inhibitory signal from the PC (e, right). The color of the frames corresponds to the color of structure in the Panel a. **f)** DCN activation plotted in a polar coordinate. Activation across the population of cells results in a vector (purple

arrow) indicating the change in hand angle (Δ hand). Note that the vector points in the same direction as the error (c, left), and thus serves to compensate for the error.

Behavioral Task and Model Parameterization

In the following sections, we evaluate the CPC model, asking how well it captures a range of phenomena observed during sensorimotor adaptation in various environments and under various training schedules. For the empirical studies, we use a visuomotor rotation task in which the visual feedback during a reaching task is limited to a cursor. To isolate cerebellar-dependent sensorimotor adaptation, we used task-irrelevant clamped feedback in which the radial position of the cursor is locked to the hand, but the angular position is predetermined for each trial, shifted by a constant angle relative to the target (Fig. 2a-b)[5]. Despite being fully informed of the non-contingent nature of the feedback and instructed to ignore the feedback, the reach angle gradually shifts in the opposite direction of the clamp[5,15,38,39]. Clamp-induced adaptation has all of the hallmarks of implicit adaptation and, as with other forms of this type of learning, is dependent on the integrity of the cerebellum[5,40].

In Exp 1, we used a clamp with a fixed angle of 30° during a 100-trial training phase followed by a 60-trial no-feedback "washout" phase (Fig 2c). The CPC model provides an excellent fit of the entire learning function (Fig 2c). Notably, even with this very simple training schedule, a basic state-space model[38,41], the most widely used model of sensorimotor adaptation, is unable to simultaneously capture the learning and forgetting phases (Fig 2c-d, also see Supplemental Result 1).

The data from Exp 1 were used to determine three parameters in the CPC model: The learning and forgetting rates for plasticity at the DCN, and the scaling factor, a parameter that transforms neural activation into hand angle. The other two parameters of the model, learning and forgetting rates for

plasticity at the PCs, were empirically estimated in Exp 6 (see below). All five parameters were fixed in the model simulations for the other experiments.

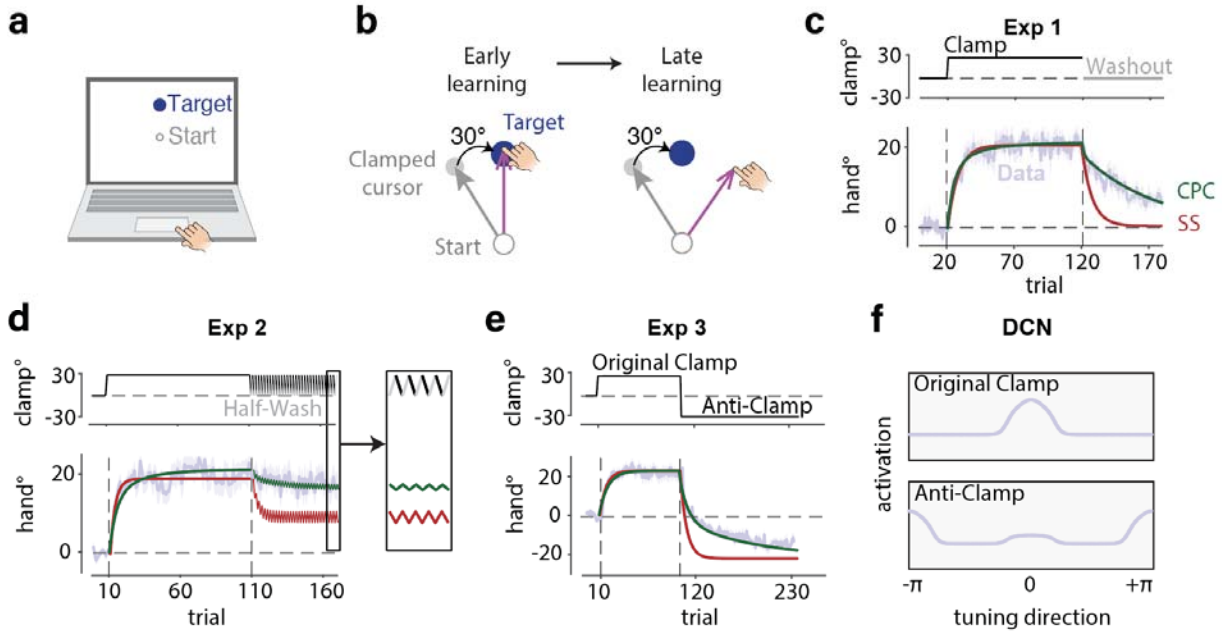

Fig. 2 Cerebellar population coding captures learning, forgetting, and anterograde interference during implicit adaptation. a) For online testing, stimuli are presented on the participant's laptop computer and movements are made on the trackpad. **b)** For clamped feedback, the angular position of the cursor is rotated by 30° with respect to the target, regardless of the heading direction of the hand. For a 30° clockwise clamp, the error direction remains at 0 on all trials. Similarly, for a -30° rotation (counterclockwise), the error direction would be invariant at π. **C)** Perturbation schedule (top) and results (bottom) for Exp 1. Time course of hand angle is shown in light violet. The CPC model provides a good fit in both the training and no-feedback washout phases. The state-space (SS) model using parameters fit from the training phase overestimates the forgetting rate in the washout phase. **d)** In Exp 2 (detailed in Supplemental Result 1), half washout phase entails a 50/50 mix of clamp and no-feedback trials. Consistent with the CPC model, hand angle showed a small reduction whereas the state-space model predicts the hand angle will be reduced by 50%. **e)** We reversed the clamp direction during the training section of Exp 3. The behavioral results match the prediction of the CPC. **f)** Memory of the original perturbation (top row) persists in the anti-clamp training phase, indicated by the activation of neurons tuned to 0 in the bottom row. This residual memory causes anterograde interference. Note that all of the model parameters were fixed in generating the predictions for Exps 2-3. Shaded area in c, d, e indicates standard error.

Anterograde Interference

Having shown that the CPC model can capture the basic features of sensorimotor adaptation, we now turn to phenomena in which adaptation is influenced by the experimental context. For units aligned with a specific error, synaptic strength undergoes rapid changes due to the potent impact of complex spikes. However, the recovery or resetting of these synapses during washout follows a relatively slow decay. As such, at the population level, the net output of the system will be influenced by the persistent state of units that were tuned to a recent perturbation. For example, due to this persistent state, the rate of adaptation should be attenuated when the system is presented with a perturbation in the opposite direction of a recently experienced perturbation. This effect is known as anterograde interference and has previously been shown to occur during implicit adaptation[42–46].

To examine whether our model can quantitatively predict anterograde interference using the parameters measured from previous experiments, we used a task in which the sign of the clamp was immediately reversed after an initial training block (e.g., 30° followed by -30°, Exp 3, see Fig 2e). The results showed that the rate of adaptation was slower in response to the reversed clamp compared to the original clamp. Indeed, the degree of attenuation closely matched the CPC model's prediction (Fig 2f).

Attenuation in Relearning and Absence of Spontaneous Recovery

Anterograde interference has typically been explained by positing context-dependent learning mechanisms[27,47,48]. For example, the contextual inference (COIN) model assumes that the motor system forms separate memories for different contexts and chooses which memory to use based on the inferred context[26]. To account for the results of Exp 3, COIN would first build a memory for the 30°

perturbation and then a second, distinct memory for the -30° perturbation. Anterograde interference would arise because the introduction of the -30° perturbation would lead to some degree of recall of the response to the initial perturbation. Over time, this would shift to a bias to recall the response to the second memory.

As shown in the previous section, the CPC model does not posit distinct memories for different perturbations; rather anterograde interference emerges from the dynamics of the CPC model. While CPC and COIN make similar predictions about anterograde interference, the two models make differential predictions on another memory recall phenomenon, spontaneous recovery. Spontaneous recovery refers to reappearance of a previously extinguished response, even when error information has not been re-introduced (e.g., no feedback phase). A paradigmatic design to elicit spontaneous recovery in sensorimotor learning studies would be to train participants with a perturbation in one direction, extinguish the adapted behavior by shifting the perturbation in the opposite direction, and then test movements without feedback (Fig 3a). Spontaneous recovery refers to the fact that the initial movements during the no-feedback phase are in the opposite direction of the initial perturbation (Fig 3c left). By the COIN model, spontaneous recovery occurs because of recall of the original context during the no-feedback phase. In contrast, the CPC model predicts that spontaneous recovery will not occur when learning is restricted to the implicit system since the model does not have a mechanism for context-dependent memory (Fig 3c right).

In Exp 4, participants were trained with a 30° clamp in one direction for 100 trials and then presented with the opposite clamp for 15 trials (Fig 3a). Pilot testing had shown that this was sufficient to extinguish the shift in hand angle observed to the initial perturbation. The critical test was the

subsequent 30-trials no-feedback block. At odds with the prediction of COIN, we failed to observe spontaneous recovery (Fig 3c, see Fig S1b).

A second point of contrast between the CPC model and context-dependent models such as COIN can be obtained by re-introducing the initial perturbation after the no-feedback washout (Fig 3a, relearning). The COIN model predicts that relearning should be faster (i.e., exhibit savings) because the system has stored a memory of the initial perturbation. The CPC model predicts that exposure to the opposite error during the washout phase will induce anterograde interference; as such, relearning will now be attenuated. Again, the results support the CPC model: Adaptation during the re-exposure block was slower compared to initial learning (Fig 3e; Fig S1a).

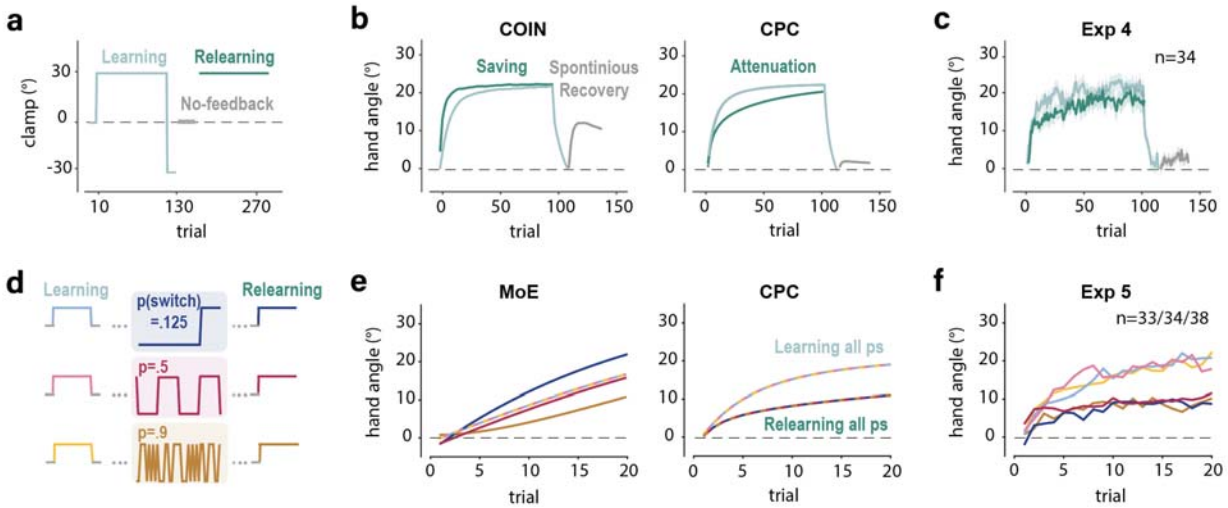

Fig. 3 Context as an emergent property of the CPC model. a) Exp 4 perturbation schedule. The learning and relearning phases are separated by an anti-clamp washout and no feedback phase to examine spontaneous recovery. The original perturbation is reintroduced in the second learning phase to test for savings. **b)** The COIN model predicts spontaneous recovery and savings; the CPC model predicts no spontaneous recovery and attenuation upon relearning. Note that, for visualization, the data from the relearning phase are plotted on top of the original learning phase. **c)** Empirical results match both predictions of the CPC model. Shaded area in c indicates standard error. **d)** In Exp 5, the learning and relearning phases are separated by a variable

phase in which the probability of a perturbation switch is manipulated between participants. **e)** The MoE model predicts that during relearning, the learning rate will be modulated by the prior switching rate (i.e., perturbation variability) whereas the CPC model predicts that the learning rate will not be modulated by switching rate. **f)** Empirical results are in accord with CPC model, showing attenuation and insensitivity to switching rate.

Insensitivity to Error Consistency

Context-dependent models confer a degree of flexibility on a learning process; in the case of COIN, the system is capable of storing multiple context-specific memories. An alternative form of flexibility is to allow the parameters of the model to change in response to context. For example, the Memory of Error (MoE) model assumes that the sensitivity of the system is modulated by error history[49]. Specifically, learning rate increases when the experienced errors are consistent and decreases when the experienced errors are inconsistent. Such a property is functionally useful in that the system will learn faster when the environment is relatively stable.

The CPC model does not provide such flexibility. Rather, we posit that the model parameters are fixed and experience-dependent changes in the response to an error arise because previous errors have transiently altered the state of the system. To compare the MoE and CPC models, we tested the response to a clamp with a fixed sign (e.g., 30°) before and after a block in which the sign of the clamp varied, with the switching probability set to 12.5%, 50%, or 90% (Fig 3d). The MoE predicts that the rate of relearning will be modulated by the switching frequency (Fig 3e left). However, consistent with the predictions of the CPC model, the rate of relearning was independent of the switching frequency (Fig 3e-f). Interestingly, relearning was markedly slower than the original learning (Fig S1c). This attenuation is another manifestation of anterograde interference resulting from the opposite errors experienced in the variable-clamp block.

These phenomena have been previously explained as reflecting the operation of multiple processes that operate at different learning rates.[36,50] However, by the CPC model different learning rates can be an epiphenomenon of population coding rather than reflect the joint operation of multiple learning mechanisms (Fig S2). Cells with a preferred direction centered on the error direction will display relatively fast learning and quickly saturate. In contrast, cells with a preferred direction slightly misaligned with the error direction will learn slower due to the weaker climbing fiber input and take longer to saturate. The behavior change in movement direction is dictated by all of the units.

The CPC model provides a novel account of another phenomenon described in the adaptation literature, namely that behavior reflects the summed activity of multiple learning processes that operate at different rates.[36,50] Here we show that this can be an epiphenomenon of population coding rather than reflect the joint operation of multiple learning mechanism (see Fig S2).

Variation in Temporal Dynamics of Different Learning Processes

The preceding sections have focused on one critical feature of the CPC model, the population effects that emerge when individual units code both movement and error direction. We now turn to the other key feature of the model, that cerebellar-dependent learning involves an interaction between plasticity effects occurring in the cerebellar cortex and deep cerebellar nuclei, with the former gating the learning rate of the latter.

Our starting point here comes from an adaptation protocol in which the sign and size of the perturbation randomly varies across trials. Consistent with previous studies[5,51,52], the response to clamped feedback in this design (Exp 6) scaled for perturbations up to around 30°, and then saturated or even slightly decreased for larger perturbations (Fig 4a). Importantly, when we empirically estimate

forgetting (see Methods), the retention rate is close to 0.5, indicating that about half of the learning from the previous trial has been forgotten. This value stands in marked contrast with the empirically estimated retention rate from designs in which the perturbation is fixed (Exp 1, 0.98). This difference is also found in previous studies using either variable perturbations in a trial-by-trial design[52–54] or a fixed perturbation in a block design[39] (Fig 4b,c).

The discrepancy in forgetting rates for blocked vs variable designs could be taken to indicate that perturbation variability influences adaptation. However, given the results of Exp 5 (see also [55]), we consider an alternative hypothesis, namely that implicit adaptation entails at least two processes that operate on different timescales[18,50]. One process is labile, driving rapid changes that are weakly retained. The other process is stable, producing changes at a relatively slow rate but with good retention (Fig 4h, Fig S3).

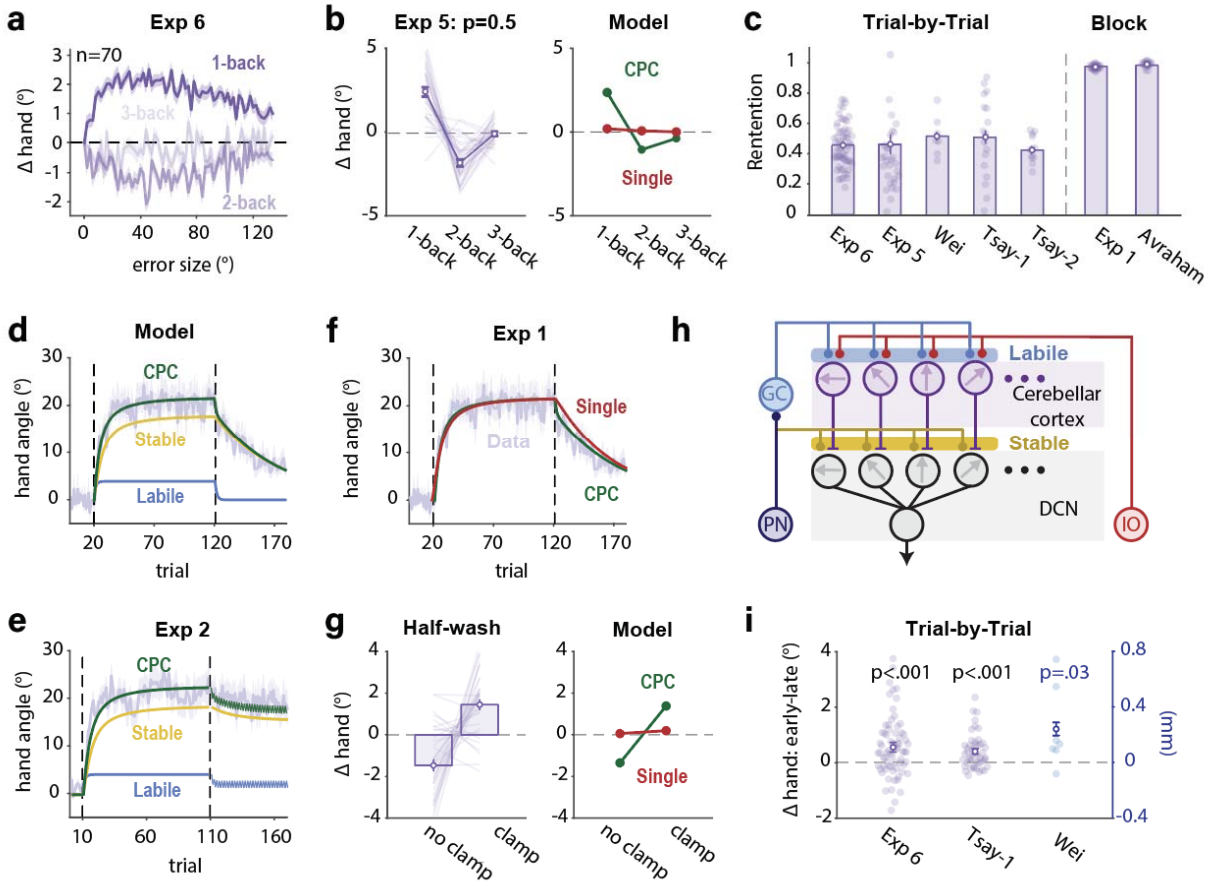

Fig. 4 Operation of labile and stable processes in cerebellum-dependent adaptation. a) Trial-by-trial change of hand angle (Δhand) as a function of the perturbation size on trial n-1 (1-back), n-2 (2-back), and n-3 (3-back) of Exp 6. **b)** Left: Δhand during variable phase of Exp 5 for the 50% switching condition. Right: The two-layer CPC model can account for the large change in hand angle observed in trial-by-trial designs whereas a single-layer model predicts a negligible change when the perturbation direction is varied. The forgetting rate can be empirically measured as the ratio between the Δhand of the 1-back and 2-back trials. **c)** Retention rate in the variable perturbation conditions is close to 0.50 whereas the retention rate in response to a fixed perturbation is close to 0.99. Re-analysis of data from Wei: [52]; Tsay-1: Exp 2 [53]; Tsay-2: Exp 3 [56], Avraham: Exp1 [39]. In all situations (trial-by-trial and blocked), we only included experiments tha used a single target. **d-e)** Simulated time course of the stable and labile processes in Exp 1 (d) and Exp 2 (e), along with their summed effect on behavior (CPC), and behavioral results. **f)** A single-layer model fails to account for the rapid forgetting observed at the start of the washout phase in Exp 1. **g)** The large Δhand in the half washout phase of Exp 2 (left) can only be accounted for by the two-layer CPC model (right). **h)** The labile process is hypothesized to produce LTD at the parallel fiber-PC synapse; the stable process is hypothesized to produce LTP at the mossy fiber-DCN synapse. **i)** As predicted by the two-process CPC model, when exposed to a

variable perturbation, the Δhand is larger in early training compared to late training. Shaded areas and error bars indicate standard error.

The dual operations of stable and labile learning processes is evident in other features of our data. In Exp 1, the retention rate changed over the course of the no-feedback block (Fig 4d), with large forgetting over the initial washout trials and much slower forgetting over the remainder of the block (also see Exp7, Fig S4). Fitting the results requires the joint operation of two forgetting rates operating at different temporal scales (Fig 4e). Moreover, in the half-washout condition of Exp 2, there is a considerable drop in hand angle after each no-feedback trial and a considerable increase after each clamp trial with a net result that the asymptote remains largely unchanged (Fig 4f, g). The large trial-by-trial change of hand angle near asymptote clearly suggests the operation of a labile process on top of a saturated stable process. Furthermore, with a variable perturbation, the learning rate is faster at the start of learning and decreases over the course of training (Fig 4i). Consistent with the CPC model, early learning reflects the operation of both the labile and stable processes, whereas during late learning, the stable process is saturated and performance changes are driven solely by the labile process (Fig S5).

<u>Learning of the Stable Process is Gated by the Labile Process.</u>

Having seen that a two-process model is required to capture adaptation, we next consider the relationship between the labile and stable processes. In particular, do they make independent contributions to adaptation, or do they interact? As outlined above, the CPC model proposes a specific form of interaction, namely that the stable process is gated by the labile process, with the former characterizing plasticity in the DCN and the latter plasticity in PCs (Fig 4h). This proposition is motivated by anatomical and physiological considerations: Anatomically, the output of the PCs provides the primary input to the DCN. Physiologically, learning in the cerebellar cortex occurs over a shorter time

scale compared to the DCN[22,32,36,57,58]. Given this two-layered network, we should find that the learning rate in the DCN is scaled by the change in simple spike activity of the PCs.

As a first test of this hierarchical organization, we asked whether the stable and labile processes are modulated in a similar way by perturbation size. Given the hierarchical assumption of the CPC model, we should be able to measure the learning rate of the labile process with a variable perturbation design (Fig 5a) and use this to predict learning functions in response to fixed perturbations of different size. Alternatively, if the stable and labile processes are independent, then we should not observe a similar yoking. We considered two variants of an independent model (Fig 5b), one in which the learning rate of the stable process is invariant across error size (FIX model) and one in which it is proportional to error size (LINEAR model).

Consistent with the CPC model, using the estimates of the labile learning rate from Exp 6 (Fig 5a), we were able to predict the learning functions in response to an invariant clamp of either 3° or 30° (Exp 8, Fig 5c). The two alternative models (FIX and LINEAR) fail to account for the data (Fig 5d). Specifically, the learning curves diverged during the early phase of learning before converging in late learning. When expressed as the ratio of hand angle in response to the large perturbation relative to the small perturbation, we observe a function that peaks early before dropping in a gradual manner (Fig 5e). We performed a similar analysis on other data sets that involved a comparison of different error sizes[51] and found a similar pattern (Fig S6b-c).

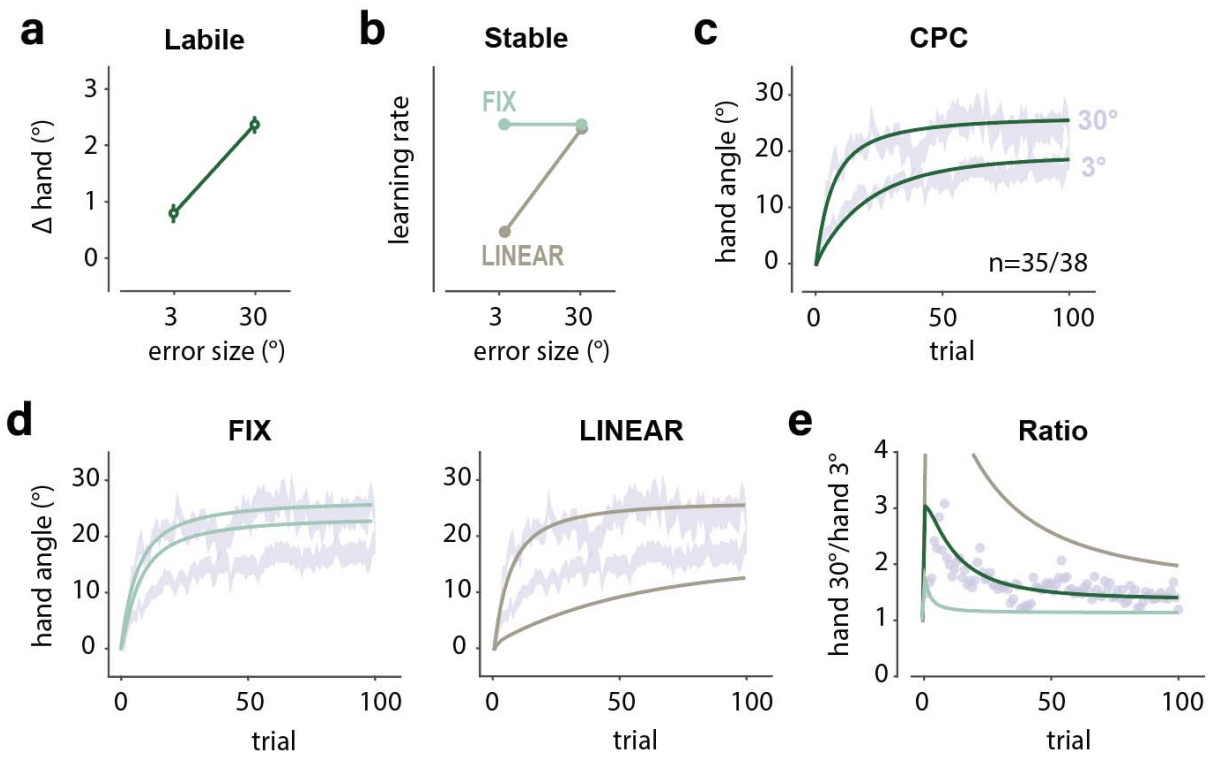

Fig. 5 Labile and stable learning rates are modulated in a similar manner by error size. a) The effect of error size on the labile process measured in Exp 6. For the CPC model, the ratio of the Δhand in a was used to estimate the learning rate of the stable process for the 3° condition (all other parameters are the same as in the 30° condition). **b)** Two alternative models in which the labile and stable processes are independent: In one, the learning rate of the stable process is invariant (FIX model) and in the other, the learning rate of the stable process is proportional to error size (LINEAR model). **c)** The CPC model (green) was able to predict the learning functions in response to both a small and large fixed perturbation (light violet). **d)** The FIX and LINEAR models fail to predict the learning curve in the 3° condition. **e)** The hand angle ratio for the two error sizes. Early in learning, the ratio is large and then converges to a value slightly larger than 1. The best fitting model assumes that the labile and stable processes are modulated in a common manner, a signature of a system in which one signal gates the other. Shaded area and error bar indicate standard error.

In a second test of the gating hypothesis, we manipulated the duration of the inter-trial interval. The trial-by-trial change in hand angle arising from the labile process should decrease with the passage of time (Fig 6a). If this process gates the learning rate of the stable process, increasing the ITI should also

decrease the learning rate of the stable process (Fig 6b left). Alternatively, if the two processes operate in parallel (PARALLEL model), the operation of the stable process should not be influenced by variation in ITI (Fig 6b right).

To evaluate these predictions, we first used a trial-by-trial design (Exp 9) to measure the change in hand angle when the ITI was short (0s) or long (7s). As predicted the change was attenuated in the 7s condition (Fig 6a). We then used a block design with either the short or long ITI (Exp 10). We ignored the first 5 trials because these would still have a contribution from the labile process. Focusing on trials 6-10, we found that the learning rate was higher in the short ITI condition, consistent with the prediction of the CPC model (Fig 6d). Moreover, the long ITI condition showed a smaller retention in early washout but not in late washout (Fig 6e), supporting the idea of the two learning processes.

However, the CPC model fails to capture one prominent feature in these data, the convergence of the two functions at asymptote (Fig 6c & f). The basic CPC predicts that the advantage for the short ITI condition should hold for the entire experiment, resulting in a lower asymptote for the long ITI condition. To address this discrepancy, we modified the CPC model (Fig 6g), adding a recurrent suppression pathway from the DCN to the inferior olive[59,60]. This inhibitory signal will reduce the strength of the error signal to the PCs[61]. If we assume that the strength of this suppression decays across the ITI, the revised CPC generates learning functions that provide good fits in both ITI conditions (Fig 6h & i, Fig S7). Importantly, after re-estimating all parameters using this variant of the CPC, we observed negligible effects on the predictions reported for the other experiments (Fig S8).

The revised CPC model can also account for another classic learning effect, contextual interference. Contextual interference refers to the phenomenon in which performance gains are slower when training

in multiple contexts compared to training in a single context, but retention is better in the former[62,63]. This phenomenon, at least in the context of implicit adaptation, is an emergent property of the parallel operation of labile and stable learning processes (see Supplementary result 2).

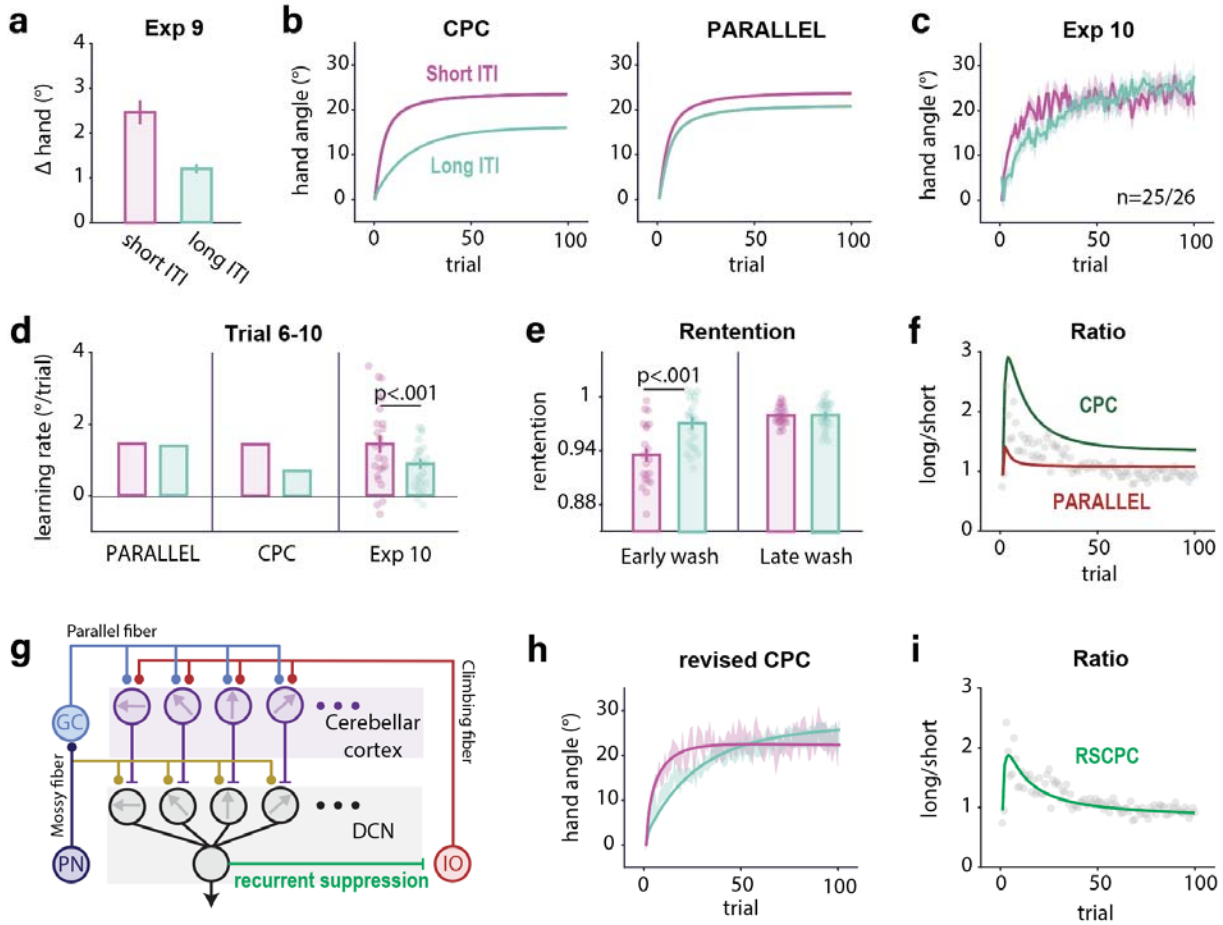

Fig. 6 The learning rate of the stable process is gated by the labile process. a) Trial-by-trial change in response to a variable perturbation with a short (Exp 5, p=0.5) or long ITI (Exp 9). **b)** Predictions of learning functions under the gating assumption of the CPC model and alternative model in which the two processes operate independently (PARALLEL). **c)** Learning functions in Exp 10 using either a short or long ITI. Consistent with the CPC model, the difference between the two functions is reduced over time. **d)** Model predictions and results from Exp 10 for the learning rate for trials 5-10. The learning rate is higher in the short ITI condition. **e)** The retention rate is larger in the initial no-feedback trials in the long ITI condition since the labile process is weakened by the passage of time. However, the retention rate is similar across the two ITI conditions later during washout, consistent with the hypothesis that only the stable process remains

operative. **f)** Hand angle ratio between short ITI and long ITI condition deviates from predictions of both models. The ratio falls between the two model predictions early in training and is smaller than predicted by both models late in training. **g)** Revised CPC model includes inhibitory projection from DCN to the IO. This suppresses the error signal conveyed by the climbing fibers. This suppression is assumed to decay with time, becoming negligible in the long ITI condition in the revised CPC model. **h-i)** Predictions of the revised CPC model provide a good fit to the learning curve (h) as well as the change in the ratio between the long and short ITI conditions (i) in Exp 10. Shaded area and error bar indicate standard error.

Discussion

To support flexible behavior, an organism needs to choose an action appropriate for a given context and execute a movement to achieve the desired outcome. A large body of work has sought to delineate the principles of these learning processes, with one prominent question centering on how the processes incorporate context and respond to uncertainty. Here we address this question with respect to the cerebellum, a subcortical structure long recognized as essential for keeping the sensorimotor system precisely calibrated in the face of fluctuations in the environment or state of the agent. We developed a population-coding model incorporating two key features: 1) Units are tuned to both movement direction and error direction, and 2) learning occurs at different rates in the cerebellar cortex and deep cerebellar nuclei, with the former characterized by a fast, labile process and the latter characterized by a slower, stable process. Our CPC model provides a parsimonious account of a diverse range of learning phenomena and offers new insight into the temporal dynamics of learning (Table S1).

Context Dependency as an Emergent Property of Population Coding

Importantly, there is no explicit role of context in the CPC model in the sense that a context does not trigger the retrieval of its associated response. Rather the signatures of context-dependent learning and environmental uncertainty emerge naturally from a population of tuned elements that operate in an inflexible manner. In this way, the CPC model diverges from classic models in the behavior that emerges

when a previously encountered context is re-experienced. Under such circumstances, classic models predict savings in relearning given that the context facilitates the retrieval of the appropriate response[26]. In contrast, the CPC model accounts for the fact that when a previously experienced perturbation is encountered, implicit adaptation not only fails to show savings, but actually can show attenuation[15]. This attenuation can be seen as another manifestation of anterograde interference: Due to the tuning properties of neurons in the cerebellar cortex and DCN, persistent activation in response to error in one direction will interfere with the response to an error in a different direction.

Given the impressive flexibility in human motor learning, it might be surprising that implicit adaptation does not explicitly track the context or uncertainty of the environment[26,47,64]. We propose that this rigidity reflects a degree of modularity between processes associated with action selection and those related to movement implementation. The cerebellum is part of a system designed to use error information to ensure the accurate execution of a desired movement. The emphasis here is on "desired movement" rather than "planned action" to underscore the point that this system appears to operate independent of the task goal; indeed, participants will adapt to sensory prediction errors even when the change in behavior is detrimental to task success[5,8]. This modularity provides a means to keep the system properly calibrated across changes in the internal state of the organism (e.g., perceptual biases, fatigue), factors that need not require a change in action planning. In contrast, other learning systems are designed to use error information related to task success to determine if the selected action was optimal given the current context. These systems would be optimized to track contextual shifts in determining the appropriate policy. Consistent with this hypothesis, contextual effects such as savings and sensitivity to uncertainty are observed in adaptation tasks that benefit from changes in action selection[49,68,69].

Hierarchical Organization Within the Cerebellum for Implicit Adaptation

The behavior observed in adaptation studies is assumed to reflect the function of learning processes that operate at different time scales[18,70]. It has been suggested that fast and slow processes correspond to explicit and implicit learning processes[71]. By using trial-by-trial and block designs, we provide evidence that learning limited to just the implicit system operates at different timescales. However, rather than view these as processes that operate in parallel, our empirical and modeling results highlight a hierarchical organization in which accumulated learning from a labile process will constrain the learning rate of a stable process. This organization readily maps onto a two-layered network formed by the cerebellar cortex and DCN, with the output from the former gating learning within the latter. The neurophysiological evidence is consistent with this assumption. While the change of SS activation in the PCs can happen within a few trials[22,63], changes within the DCN can maintain learning across days[25,38]. Reflective of the hierarchical organization, we showed that there is an asymmetric dependency such that the synaptic strength in the cerebellar cortex determines the PC output that modulates learning within the DCN.

We recognize that a two-layered model is clearly a simplification. Indeed, to explain the asymptotic convergence in the long and short ITI conditions, we had to incorporate a third layer into the model, creating a closed loop by adding a projection from the DCN to the IO. While the anatomy supports the existence of this pathway, to achieve convergence, we added two specific features to the dynamics of this pathway. First, inhibition from the DCN to the IO exhibits a unique temporal dynamic, with its intensity decreasing over time. Second, the projection is generic, inhibiting IO units independent of the directional tuning of the DCN neuron. These two assumptions need to be tested in future physiological studies.

Generalization of the CPC model

Though our model focuses on the cerebellum and sensorimotor learning, the core computational principles may offer insight into how the nervous system responds to environmental uncertainty. The population-coding aspect of the CPC model is similar to models of perceptual learning that include a basis set of tuned elements[74]. For example, in models of time perception, contextual effects on perceived duration have been proposed to reflect the interaction of units tuned to different durations[75,76]. Applied to this domain, the CPC model could be used to derive specific predictions of how temporal perception is modulated by uncertainty and establish boundary conditions for interference. Moreover, the two-layer network in the CPC model provide a novel framework to understand of how learning can involve multiple processes that follow different temporal dynamics, a phenomenon widely observed in cognitive tasks. For instance, value learning has been hypothesize to reflect the joint operation of a fast, volatile process and a slow, stable process[63]. While these processes are typically viewed as operating in parallel, the CPC model offers an example of how a hierarchical framework might prove more parsimonious.

Methods

Cerebellar Population Coding (CPC) model

Here we extend the classic Marr-Albus model, focusing on how learning is modulated when the environment is variable. A foundational idea for our model is inspired by a recent work showing how PCs in the oculomotor cerebellar cortex are simultaneously tuned to both movement direction and the error that is associated with that movement [22,23].

To examine the implications of these tuning properties for cerebellar-dependent learning, we incorporate PC tuning into a learning model. Specifically, we formalize the teaching signal, the complex spike (CS) activity of a PC with a preferred direction of i ($0 \leq i < \pi$) in response to a movement error e (Fig 1d) as:

$$[1]\ CS_i^n = VM(\theta^e, i, s)\mathrm{F}(\rho^e)$$

where $VM(\ i, s)$ is the probability density function of a simplified circular (von Mises) distribution with a mean of i and standard deviation of s. θ^e and ρ^e refer to the direction and the size of e, respectively, and n is the trial number. F is a non-linear function, reflecting the well-established fact that the motor correction does not scale with error size [36,37]. The form of this non-linear relationship is not relevant in the experiments with a fixed perturbation; for those experiments, the exponent was set to 1.

Following the Marr-Albus model, the occurrence of a CS suppresses the strength of the parallel fiber input synapse (w) through long-term depression (LTD):

$$[2]\ w_i^{n+1} = -lCS_i^n + f(w_\mathrm{o} - w_i^n) + w_i^n$$

where l ($l > 0$) and f ($0 < f < 1$) are the learning and forgetting rates, respectively, and w_o is the baseline synaptic strength. Since the level of single spike (SS) activity will be greatest for cells coding a

movement direction opposite to the error, the modulation of synaptic strength will drive the next movement in a direction that corrects for the observed error.

The preceding paragraph describes how parallel fiber synapses onto PCs are modified. A second prominent site of plasticity is at deep cerebellar nuclei[25,38]. Importantly, PC and DCN neurons are organized such that they share the same tuning direction for movement[43]. We posit that learning at the DCN is gated by learning at the cerebellar cortex. Specifically, LTD at parallel fiber-PC (PF-PC) synapses will reduce inhibitory PC input to the DCN, resulting in long term potentiation (LTP) at the mossy fiber-DCN synapses (m) (Fig 1e):

$$[3]\ m_i^{n+1} = (w_{\mathrm{o}} - w_i^n)ß(m_{\max} - m_i^n) + \alpha(m_{\mathrm{o}} - m_i^n) + m_i^n$$

where ß and α are the learning rate and the forgetting rate of the DCN input synapse, respectively. The parameters m_{o} and $m_{\max}$ represent baseline and maximal synaptic strength, respectively. The latter constraint is based on empirical results showing that implicit adaptation saturates independent of the error size.

Considering the two sites of plasticity, DCN activity on a repeated trial following a movement error can be formalized as:

$$[4]\ DCN_i^{n+1} \propto m_i^{n+1} - \gamma w_i^{n+1}$$

where $\gamma$is a scaling factor. The output of the population of DCN neurons will correspond to the change in movement direction in response to an error, a signal that can be used to adjust the movement. This can be expressed as: (Fig 1f):

$$[5]\ \boldsymbol{h}^{n+1} = -\varepsilon \sum_i \boldsymbol{v}_i DCN_i^{n+1}$$

where $\boldsymbol{h}^n$ is a vector representing the hand angle on trial n, $\boldsymbol{v}_i$ is a vector representing the tuning direction of unit i, and ε is a scaling factor to transfer the neural activity into hand angle.

We note that we do not specify, for the purposes of this paper, whether the cerebellum is best viewed as a forward or inverse model. The current implementation of the CPC model most resembles an inverse model given that the system modifies the motor commends based on the error. However, the model could be reframed as a forward model with the output a prediction that is fed into an (cerebellar or extracerebellar) inverse model that refines the motor commands

Parameterization of the CPC Model

We used an empirical approach to estimate the learning and forgetting rate for PF-PC synapses, using the data from Exp 5 in which +/- $30°$ clamps were presented with a 50% switching probability. To measure single trial learning, we calculate the change of hand angle between trial n and trial n-1, flipping the sign when the clamp on trial n-1 was negative. To measure single trial forgetting, we calculate the change of hand angle between trial n and trial n-1, flipping the sign when the clamp on trial n-2 was negative.

PF-PC forgetting (f) is the ratio of single-trial forgetting and single-trial-learning. By definition, retention rate is 1- (f). We applied the same method to measure the retention for all trial-by-trial designs and this gave us an f around 0.5. Model simulations indicate that this method can precisely estimate retention when the perturbation is random. In all of these analyses, we excluded the first 50 trials since learning at this early stage is influenced by both PC and DCN. For comparing the learning rate between early and late training in a trial-by-tri

al design, we employed the same general approach but limited the analysis to the first 50 trials to estimate early learning (Fig S5).

The baseline and maximal strength of MF-DCN synapses can be set to arbitrary values: We used 1 and 1.85 for m_{o} and $m_{\max}$, respectively. We measured the retention rate of the MF-DCN synapse (α) empirically using the data from the no-feedback washout phase in Exp 1:

$$\alpha = \sqrt[10]{mean(\frac{y^{n+10}}{y^{n}})}$$

where y^{n} is the hand angle in trial n. The first 20 trials in the washout phase were excluded since they may be contaminated by a labile process.

The learning rate of the PC (l) and DCN (ß) and the scaling factors (γ, ε) were jointly fitted from the learning block in Exp 1 and the single trial learning in Exp 5. This results in a parameter set as follow: l = .05, f = .018, ß = 2, α = .5, γ= 0.15, ε = 130. These parameters were fixed in the simulations of all the other experiments. The two exceptions are mentioned below.

First, in Exp 7, we examined how error size modulated learning using a block design in which the clamp was at 3° or 30° clamp in separate conditions (between-subject). The prediction for the 30° clamp condition was generated based on the parameter set described above. For the 3° clamp, we applied a scale factor of 0.33 on CS activation:

$$[6]\ cs(3°) = 0.33 * cs(30°)$$

This value was based on the empirically observed values for 3° and 30° clamps in the trial-by-trial design of Exp 6. Second, in Exp 10, we set the PF-PC retention rate for the long ITI conditions (f') to be 0.3, based on the empirically observed value in the trial-by-trial design of Exp 9.

Revised CPC model

The results of Exp 9 led us to develop a post-hoc variant in which the output of the cerebellum modulates the input, an idea that is consistent with cerebellar anatomy and physiology[59,60]. The basic version of the CPC model predicts that learning in a long ITI condition will reach a lower asymptote compared to a short ITI condition. This occurs because the contribution of the labile process is suppressed in the long ITI condition. However, the results of Exp 10 showed that, with a sufficient number of trials, learning in the long ITI condition eventually reaches the same asymptote as in the short ITI condition. This observation led us to revise the model by adding an inhibitory pathway from the DCN to the inferior olive[59,60]., what we will refer to as the cerebellar population coding model with recurrent suppression.

We assume that the output of the DCN integrates the activation of directionally tuned units and that this signal serves as a generic inhibitory signal to the inferior olive. We implemented this recurrent suppression by subtracting a common value from the activation of cells tuned to all error directions in the inferior olive (IO):

$$[8] IO_i = 1 - \omega * \sum_i dDCN_i^n$$

$$[9] \text{ if } IO_i > 0: cs'_i = IO_i * cs_i;$$

$$\text{otherwise: } cs'_i = 0$$

where ω represents the strength of suppression. Given the assumption that ω decreases across time, we used separate parameter values of ω for the long and short ITI conditions $\sum_i dDCN_i^n$ is the sum of the change of all NCD units relative to their baseline activities. cs'_i is the corrected CS activation value after taking the DCN-IO pathway into the consideration and replaces the cs_i term in EQ [1-5]. The retention rates of the labile and stable processes (f, α) in the revised CPC model were set as in the basic

two-layer model. The other parameters (l, ß, ε, ω) were jointly fitted from two data sets, the learning block in Exp 1 and the trial-by-trial condition in Exp 9. The parameter set is as follow: l = .1, f = .018, ß = 2, α = .5, γ = .2, ε = 210, $\omega(short)$ = 2.5, $\omega(long)$ = 0.

Alternative Models for Comparison

Variants of the CPC Model

To help clarify the importance of a two-layer model, we describe two variants of the CPC model. First, we implemented a single-layer version of the CPC model by modifying Eq 4 to:

$$[7]\ DCN_i^{n+1} = m_i^{n+1}$$

In this version, the output of the system is solely determined by the strength of the MF-DCN.

Second, we implemented a model in which the labile and the stable processes operate in parallel (PARALLEL) rather than hierarchical as in the CPC model. Since the stable process is insensitive to ITI, we estimate the MF-DCN synapse (m) by simulations using a short ITI. The simulated value was then used in simulations of the long ITI condition. For the labile process, the strength of the PF-PC synapse (w) was measured separately for the two ITI conditions.

State-space model

We employed a standard version of a state-space model[18,41]:

$$[10]\ x(n+1) = a * x(n) + b(e,n)e(n) + \varepsilon_x(n)$$

where x is the internal estimate of the motor state (i.e., the hand movement required to compensate for the perturbation), a is the retention factor, $e(n)$ is the size of the perturbation in trial n, b is the error sensitivity for a given error size, and ε_x represents planning noise.

The actual motor response on trial n is given as:

$$[11]\ y(n) = x(n) + \varepsilon_y(n)$$

where y is the reaching direction relative to the target, determined by $x(n)$ and motor noise, ε_y .

Memory-of-Error model (MoE)

The Memory-of-Error model describes how the learning rate in the state space model is modulated by experience. In the MoE model, error sensitivity (b) is set to an initial value that is modulated by errors that are experienced during training. Specifically, *b(e,n)* will increase if the error on trial n+1 shares the same sign and *b(e, n)* will decrease if the error on trial n+1 is of the opposite sign. This is formalized as:

$$[12]\ b(e(n), n+1) = \alpha * (b(e(n), n+1) - b0) + b0 + \beta * sign(e(n) * e(n+1))$$

where β and α are the learning rate and retention rate of b, respectively. Since the error size is fixed at 30° in our experiments, we replace $b(e)$ with a single value b.

Contextual Inference (COIN) model

We simulated the Contextual Interference (COIN) using the code provided by Heald et al.[26], focusing on its prediction with respect to savings and spontaneous recovery. We assumed that the introduction of a perturbation (e.g., clamped feedback) defines a new context and, as such, leads to the establishment of a new motor memory. Similarly, reversing the sign of the perturbation would define another context and thus require establishment of another memory. We simulated the clamps as if they were contingent rotations so that the learning can reach an asymptote. Before each movement, the output is determined by averaging the state of different contexts weighted by the expected probabilities of the contexts. Participants observed an error after each movement and update the state estimation.

<u>Behavioral Experiments</u>

Participants

A total of 451 participants (297 female, mean age = 28.0, SD = 5.3) were recruited through the website prolific.co. After eliminating participants who failed to meet our performance criteria (2.8%, see below), the analyses were based on data from 438 participants. Based on a survey included in a prescreening questionnaire, the participants were right-handed with normal or corrected-to-normal vision. The participants were paid based on a rate of $8/h. The protocol was approved by the Institutional Review Board at the University of California, Berkeley. Informed consent was obtained from all participants.

Apparatus

All of the behavioral experiments were conducted online using a web-based experimental platform, OnPoint[56], which is written in JavaScript and presented via Google Chrome. It is designed to operate on any laptop computer. Visual stimuli were presented on the laptop monitor and movements were produced on the computer trackpad. Data were collected and stored using Google Firebase.

Clamp rotation task

We applied clamp feedback in the experiments, under the assumption that learning in response to this type of feedback is limited to implicit, cerebellar-dependent sensorimotor recalibration. To start each trial, the participant moved the cursor to a white start circle (radius: 1% of the screen height) positioned in the center of the screen. After 500ms, the target, a blue circle (radius: 1% of the screen height) appeared with the radial distance set to 40% of the screen size. The target appears at -45°, a workspace location selected because it exhibits minimal bias across participants[77]. The participant was instructed to produce a rapid, out-and-back movement, attempting to intersect the target. If the movement time

(from onset to time at which movement amplitude reached the target) was longer than 500ms, the message 'Too Slow' was presented on the screen for 500ms.

There were three types of feedback. On veridical feedback trials, the position of the cursor moved was matched to the position of the hand, subject to the translation in reference frames (screen assumed to be vertical, hand movement assumed to be horizontal) and scaling (trackpad space expanded to encompass most of the screen). On clamped feedback trials, the cursor followed a fixed path. As with veridical feedback, the radial location of the cursor was based on the radial extent of the participant's hand. However, the angular position of the cursor was independent of the position of the hand, instead determined relative to the position of the target. The clamp angle was set at 30° relative to the target except for Exp 6 and 8 (see below). On no feedback trials, the cursor was blanked at movement onset.

On veridical and clamped feedback trials, after the amplitude of the movement reached the target distance, the cursor was presented at the target distance for another 50ms then it disappeared. Target disappeared after 200ms. The cursor was then reset to a random position on an invisible circle with a radius equal to 10% of the target distance and the participant moved the cursor back to the start circle.

At the onset of the first block of trials involving perturbed feedback, the experiment was paused, and a set of instructions were presented to describe the clamped feedback. The participant was informed that the cursor would no longer be linked to their movement but rather would follow a fixed path on all trials. The participant was instructed to always reach directly to the target, ignoring the cursor. These instructions were then repeated twice to emphasize the atypical nature of the feedback. After the first 10 trials with clamped feedback, a new instruction screen appeared in which the participant was asked

to indicate where they were aiming on each trial. If the participant indicated they were reaching somewhere other than the target, the experiment was terminated.

Each experiment started with two baseline blocks: First a no-feedback block of 10 trials and second, a veridical feedback block of 10 trials. For experiments using a block design (direction and size of perturbation remain constant), the direction of the clamp (counterclockwise, CCW; clockwise; CW) was counterbalanced across participants.

Experiment 1

Exp 1 was designed to determine the parameters of the CPC model. There was a total of 180 trials. The two baseline blocks were followed by a learning block of 100 trials with clamped feedback with learning expected to reach an asymptotic level in response to a fixed perturbation. This was followed by a final no-feedback block of 60 trials. 30 participants were recruited for Exp 1 (29 valid, 5 males, age: 27.4 ± 4.9 years).

Experiment 2

Exp 2 was designed to evaluate different models of asymptotic adaptation. The 10-trial feedback baseline were followed by a learning block of 100 trials with clamped feedback. Then the last 60 trials alternated between no-feedback and clamp feedback trials (half-wash phase). 40 participants were recruited for Exp 2 (38 valid, 8 males, age: 30.7 ± 6.6 years).

Experiment 3

Exp 3 was designed to measure antegrade interference. The baseline and initial perturbation blocks were as in Exp 2. For the final block (150 trials), the direction of the clamp was reversed (e.g., from 30° to -30°). 30 participants were recruited for Exp 3 (30 valid, 10 males, age: 30.3 ± 4.3 years).

Experiment 4

Exp 4 was designed to assess spontaneous recovery and savings in implicit adaptation. The baseline and initial perturbation blocks were as in Exp 2. We then included a 15-trial block with the clamp reversed under the assumption that this would be a sufficient number of trials to bring the hand angle back to baseline. This was followed by no-feedback block (35 trials) to examine spontaneous recovery and then a 100-trial relearning block in which the clamp feedback was identical to that used in the first perturbation block. 34 participants were recruited for Exp 4 (34 valid, 16 males, age: 22.7 ± 4.8 years).

Experiment 5

Exp 5 examined how the consistency of the perturbation influenced implicit adaptation. The first blocks were identical to Exp 4, providing initial exposure to clamped feedback and then a reversed clamp to bring the hand angle back to baseline. This was followed by a 300-trial block in which the clamp changed sign in a probabilistic manner. The probability of a sign change was either 90%, 50%, and 12.5% in a between-subject manipulation. The sequence of clamps was preset to ensure that clockwise and counterclockwise occurred on 50% of the trials each across the 300 trials. The experiment ended with a relearning block in which the initial perturbation was presented for 100 trials. 36/40/36 participants were recruited for 90%, 50%, and 12.5% conditions respectively (34/38/33 valid, 37 males, age: 28.6 ± 5.5 years).

Experiment 6

To estimate the learning rate and retention at top layer of the CPC model, the PF-PC synapse, we employed a trial-by-trial design in which the error size and direction varied across trials. After the two baseline sections, participants completed a 540-trial random perturbation block. Here the clamp size ranged from -135° to 135° in steps of 1°. The size/direction was determined at random with the constraint that each clamp was selected once every 270 trials. 72 participants were recruited for Exp 6 (70 valid, 25 males, age: 26.2 ± 5.2 years).

Experiment 7

Experiment 7 was designed to measure the time course of retention during the initial washout phase. After the two baseline sections, The perturbation block consisted of 31 mini-blocks, each composed of 10 trials with clamped feedback and 10 trials without feedback (620 trials). 57 participants were recruited for Exp 7 (57 valid, 12 males, age: 28.3 ± 5.4 years).

Experiment 8

Experiment 8 examined how error size influences learning in a block design. Two groups of participants experience a 10-trial feedback baseline and a 100-trial perturbation block in which the clamp size was either 3° or 30°. 36 participants were recruited for Exp 8 (35 valid, 18 males, age: 30.8 ± 7.7 years).

Experiment 9

To quantify the temporal dynamics of labile processes, we performed a trial-by-trial design with extended inter-trial intervals (ITI) in Exp 9. For the long ITI, the interval between the end of one trial and the start of the next trial was 6s, 7s, or 8s, randomized across trials. The message "wait" was displayed on the monitor after each trial. Exp 9 included two baseline blocks and a 180-trial learning block in which a 30° perturbation was randomly selected to be either clockwise or counterclockwise, subject to

the constraint that each direction occurred four times every 8 trials. For the short ITI condition, we used the data from Exp 5 for the trial-by-trial condition (0s ITI). 28 participants were recruited for each condition (27 valid, 13 males, age: 28.1 ± 4.8 years).

Experiment 10

To understand how the labile and stable learning processes are jointly modulated by time, we perform a block design in Exp 10. We followed a similar design to Exp 1, with only one notable modification. We included a 10-trial familiarization block following the two baseline blocks to demonstrate the clamp feedback. The clamp size in the familiarization block varied from -90° to 90° across trials to show that the cursor is unaffected by the direction of hand movement. To avoid the influence of pre-exposure to the error signal on learning, the familiarization block utilized a different target (45°) from the other blocks (315°). Two groups of participants performed the task with either long ITI (6-8s) or short ITI (0s). 26 participants were recruited for each condition (51 valid, 21 males, age: 26.8 ± 4.6 years).

Data analyses

Hand angle was calculated as the angle difference a line from the start position to the target and a line from the start position to the hand position at the target radius. Positive values indicate hand angles in the opposite direction of the perturbation, the direction one would expect due to adaptation. Trials with a movement duration longer than 500 ms or an error larger than 70° were excluded from the analyses. We excluded the entire data from participants who had less than 70% valid trials (2.8% participants). Between-condition comparisons were performed with t-tests or ANOVAs. Learning and relearning were compared by paired-t-test. For all the statistical tests, we confirmed that the data met the assumptions of a Gaussian distribution and homoscedasticity.

Data and Software Availability

The data and code supporting this work are available at https://github.com/shion707/CPC.

Author contributions

T.W., R.B.I. contributed to the conceptual development of this project. T.W. collected the data, analyzed the data, prepared the figures, and wrote the initial draft of the paper, with all the authors involved in the editing process.

Acknowledgment

This study is funded by the NIH (grants NS116883 and NS105839).

Competing interests

RI is a co-founder with equity in Magnetic Tides, Inc.

References

1. Ito, M. Mechanisms of motor learning in the cerebellum. *Brain Res.* **886**, 237–245 (2000).
2. Albus, J. S. A theory of cerebellar function. *Math. Biosci.* **10**, 25–61 (1971).
3. Kawato, M. Internal models for motor control and trajectory planning. *Curr. Opin. Neurobiol.* **9**, 718–727 (1999).
4. Ebner, T. J. & Pasalar, S. Cerebellum predicts the future motor state. *Cerebellum* **7**, 583–588 (2008).
5. Morehead, J. R., Taylor, J. A., Parvin, D. E. & Ivry, R. B. Characteristics of Implicit Sensorimotor Adaptation Revealed by Task-irrelevant Clamped Feedback. *J. Cogn. Neurosci.* **29**, 1061–1074 (2017).
6. Taylor, J. A., Klemfuss, N. M. & Ivry, R. B. An Explicit Strategy Prevails When the Cerebellum Fails to Compute Movement Errors. *Cerebellum* **9**, 580–586 (12/2010).
7. Taylor, J. A. & Ivry, R. B. Cerebellar and prefrontal cortex contributions to adaptation, strategies, and reinforcement learning. *Prog. Brain Res.* **210**, 217–253 (2014).
8. Mazzoni, P. & Krakauer, J. W. An implicit plan overrides an explicit strategy during visuomotor adaptation. *J. Neurosci.* **26**, 3642–3645 (2006).
9. Taylor, J. A., Krakauer, J. W. & Ivry, R. B. Explicit and Implicit Contributions to Learning in a Sensorimotor Adaptation Task. *Journal of Neuroscience* **34**, 3023–3032 (2014).
10. Wang, T. & Taylor, J. A. Implicit adaptation to mirror reversal is in the correct coordinate system but the wrong direction. *J. Neurophysiol.* **126**, 1478–1489 (2021).
11. Wilterson, S. A. & Taylor, J. A. Implicit Visuomotor Adaptation Remains Limited after Several Days of Training. *eNeuro* **8**, (2021).
12. Avraham, G., Keizman, M. & Shmuelof, L. Environmental consistency modulation of error sensitivity during motor adaptation is explicitly controlled. *J. Neurophysiol.* **123**, 57–69 (2020).

801 13. Wang, T., Avraham, G., Tsay, J. S., Abram, S. J. & Ivry, R. B. Perturbation Variability Does Not
802 Influence Implicit Sensorimotor Adaptation. *bioRxiv* 2023.01.27.525949 (2023)
803 doi:10.1101/2023.01.27.525949.
804 14. Albert, S. T. *et al.* Competition between parallel sensorimotor learning systems. *Elife* **11**, (2022).
805 15. Avraham, G., Morehead, J. R., Kim, H. E. & Ivry, R. B. Reexposure to a sensorimotor perturbation
806 produces opposite effects on explicit and implicit learning processes. *PLoS Biol.* **19**, e3001147
807 (2021).
808 16. Denny-Brown, D. Conditioned reflexes: An investigation of the physiological activity of the cerebral
809 cortex. *Nature* **121**, 662–664 (1928).
810 17. Ebbinghaus, H. Memory: a contribution to experimental psychology. *Ann. Neurosci.* **20**, 155–156
811 (2013).
812 18. Smith, M. A., Ghazizadeh, A. & Shadmehr, R. Interacting Adaptive Processes with Different
813 Timescales Underlie Short-Term Motor Learning. *PLoS Biol.* **4**, e179 (2006).
814 19. Herzfeld, D. J., Kojima, Y., Soetedjo, R. & Shadmehr, R. Encoding of action by the Purkinje cells of
815 the cerebellum. *Nature* **526**, 439–442 (2015).
816 20. Sedaghat-Nejad, E., Pi, J. S., Hage, P., Fakharian, M. A. & Shadmehr, R. Synchronous spiking of
817 cerebellar Purkinje cells during control of movements. *Proceedings of the National Academy of*
818 *Sciences* **119**, e2118954119 (2022).
819 21. Junker, M. *et al.* Learning from the past: A reverberation of past errors in the cerebellar climbing
820 fiber signal. *PLoS Biol.* **16**, e2004344 (2018).
821 22. Carulli, D. *et al.* Cerebellar plasticity and associative memories are controlled by perineuronal nets.
822 *Proc. Natl. Acad. Sci. U. S. A.* **117**, 6855–6865 (2020).
823 23. Raymond, J. L., Lisberger, S. G. & Mauk, M. D. The cerebellum: a neuronal learning machine?
824 *Science* **272**, 1126–1131 (1996).

24. Lisberger, S. G., Pavelko, T. A. & Broussard, D. M. Responses during eye movements of brain stem neurons that receive monosynaptic inhibition from the flocculus and ventral paraflocculus in monkeys. *J. Neurophysiol.* **72**, 909–927 (1994).

25. Lee, K. H. *et al.* Circuit mechanisms underlying motor memory formation in the cerebellum. *Neuron* **86**, 529–540 (2015).

26. Heald, J. B., Lengyel, M. & Wolpert, D. M. Contextual inference underlies the learning of sensorimotor repertoires. *Nature* **600**, 489–493 (2021).

27. Haruno, M., Wolpert, D. M. & Kawato, M. Hierarchical MOSAIC for movement generation. *Int. Congr. Ser.* **1250**, 575–590 (2003).

28. Collins, A. & Koechlin, E. Reasoning, learning, and creativity: frontal lobe function and human decision-making. *PLoS Biol.* **10**, e1001293 (2012).

29. Kawato, M. Feedback-Error-Learning Neural Network for Supervised Motor Learning. in *Advanced Neural Computers* (ed. Eckmiller, R.) 365–372 (North-Holland, 1990).

30. Wolpert, D. M., Miall, R. C. & Kawato, M. Internal models in the cerebellum. *Trends Cogn. Sci.* **2**, 338–347 (1998).

31. Apps, R. & Garwicz, M. Anatomical and physiological foundations of cerebellar information processing. *Nat. Rev. Neurosci.* **6**, 297–311 (2005).

32. Moscato, L. *et al.* Long-Lasting Response Changes in Deep Cerebellar Nuclei in vivo Correlate With Low-Frequency Oscillations. *Front. Cell. Neurosci.* **13**, 84 (2019).

33. Ito, M. Cerebellar control of the vestibulo-ocular reflex--around the flocculus hypothesis. *Annu. Rev. Neurosci.* **5**, 275–296 (1982).

34. Medina, J. F., Garcia, K. S., Nores, W. L., Taylor, N. M. & Mauk, M. D. Timing mechanisms in the cerebellum: testing predictions of a large-scale computer simulation. *J. Neurosci.* **20**, 5516–5525 (2000).

35. Garcia, K. S. & Mauk, M. D. Pharmacological analysis of cerebellar contributions to the timing and expression of conditioned eyelid responses. *Neuropharmacology* **37**, 471–480 (1998).

36. Herzfeld, D. J., Hall, N. J., Tringides, M. & Lisberger, S. G. Principles of operation of a cerebellar learning circuit. *Elife* **9**, (2020).

37. Shadmehr, R. Population coding in the cerebellum: a machine learning perspective. *J. Neurophysiol.* **124**, 2022–2051 (2020).

38. Kim, H. E., Avraham, G. & Ivry, R. B. The Psychology of Reaching: Action Selection, Movement Implementation, and Sensorimotor Learning. *Annu. Rev. Psychol.* **72**, 61–95 (2021).

39. Avraham, G., Taylor, J. A., Breska, A., Ivry, R. B. & McDougle, S. D. Contextual effects in sensorimotor adaptation adhere to associative learning rules. *Elife* **11**, e75801 (2022).

40. Tsay, J. S., Parvin, D. E. & Ivry, R. B. Continuous reports of sensed hand position during sensorimotor adaptation. *J. Neurophysiol.* **124**, 1122–1130 (2020).

41. Shadmehr, R. & Mussa-Ivaldi, F. A. Adaptive representation of dynamics during learning of a motor task. *J. Neurosci.* **14**, 3208–3224 (1994).

42. Morehead, J. R. & Smith, M. The magnitude of implicit sensorimotor adaptation is limited by continuous forgetting. *Abstract. Advances in Motor Learning & Motor Control* (2017).

43. Lerner, G. *et al.* The origins of anterograde interference in visuomotor adaptation. *Cereb. Cortex* **30**, 4000–4010 (2020).

44. Brashers-Krug, T., Shadmehr, R. & Bizzi, E. Consolidation in human motor memory. *Nature* **382**, 252–255 (1996).

45. Leow, L.-A., Hammond, G. & de Rugy, A. Anodal motor cortex stimulation paired with movement repetition increases anterograde interference but not savings. *Eur. J. Neurosci.* **40**, 3243–3252 (2014).

46. Sing, G. C. & Smith, M. A. Reduction in learning rates associated with anterograde interference results from interactions between different timescales in motor adaptation. *PLoS Comput. Biol.* **6**, e1000893 (2010).

47. Heald, J. B., Lengyel, M. & Wolpert, D. M. Contextual inference in learning and memory. *Trends Cogn. Sci.* (2022) doi:10.1016/j.tics.2022.10.004.

48. Ingram, J. N., Flanagan, J. R. & Wolpert, D. M. Context-dependent decay of motor memories during skill acquisition. *Curr. Biol.* **23**, 1107–1112 (2013).

49. Herzfeld, D. J., Vaswani, P. A., Marko, M. K. & Shadmehr, R. A memory of errors in sensorimotor learning. *Science* **345**, 1349–1353 (2014).

50. Kording, K. P., Tenenbaum, J. B. & Shadmehr, R. The dynamics of memory as a consequence of optimal adaptation to a changing body. *Nat. Neurosci.* **10**, 779–786 (2007).

51. Kim, H. E., Morehead, J. R., Parvin, D. E., Moazzezi, R. & Ivry, R. B. Invariant errors reveal limitations in motor correction rather than constraints on error sensitivity. *Commun Biol* **1**, 19 (12/2018).

52. Wei, K. & Körding, K. Relevance of Error: What Drives Motor Adaptation? *J. Neurophysiol.* **101**, 655–664 (02/2009).

53. Tsay, J. S. *et al.* The effect of visual uncertainty on implicit motor adaptation. *J. Neurophysiol.* **125**, 12–22 (2021).

54. Hutter, S. A. & Taylor, J. A. Relative sensitivity of explicit reaiming and implicit motor adaptation. *J. Neurophysiol.* **120**, 2640–2648 (2018).

55. Wang, T., Avraham, G., Tsay, J. & Ivry, R. The Effect of Perturbation Variability on Sensorimotor Adaptation Does Not Require an Implicit Memory of Errors. *bioRxiv* 2022.05.30.493844 (2022) doi:10.1101/2022.05.30.493844.

56. Tsay, J. S., Ivry, R. B., Lee, A. & Avraham, G. Moving outside the lab: The viability of conducting sensorimotor learning studies online. *Neurons, Behavior, Data analysis, and Theory* (2021) doi:10.51628/001c.26985.

57. Medina, J. F. & Lisberger, S. G. Links from complex spikes to local plasticity and motor learning in the cerebellum of awake-behaving monkeys. *Nat. Neurosci.* **11**, 1185–1192 (2008).

58. Herzfeld, D. J., Kojima, Y., Soetedjo, R. & Shadmehr, R. Encoding of error and learning to correct that error by the Purkinje cells of the cerebellum. *Nat. Neurosci.* **21**, 736–743 (5/2018).

59. Best, A. R. & Regehr, W. G. Inhibitory regulation of electrically coupled neurons in the inferior olive is mediated by asynchronous release of GABA. *Neuron* **62**, 555–565 (2009).

60. De Zeeuw, C. I. & Ruigrok, T. J. Olivary projecting neurons in the nucleus of Darkschewitsch in the cat receive excitatory monosynaptic input from the cerebellar nuclei. *Brain Res.* **653**, 345–350 (1994).

61. Bengtsson, F. & Hesslow, G. Cerebellar control of the inferior olive. *Cerebellum* **5**, 7–14 (2006).

62. Tsay, J. S., Irving, C. & Ivry, R. B. Signatures of contextual interference in implicit sensorimotor adaptation. *Proc. Biol. Sci.* **290**, 20222491 (2023).

63. Collins, A. G. E. *The tortoise and the hare: interactions between reinforcement learning and working memory*. http://biorxiv.org/lookup/doi/10.1101/234724 (2017).

64. Collins, A. G. E. & McDougle, S. D. Context is key for learning motor skills. *Nature* vol. 600 387–388 (2021).

65. Herzfeld, D. J. & Shadmehr, R. Cerebellum estimates the sensory state of the body. *Trends in cognitive sciences* vol. 18 66–67 (2014).

66. Gonzalez Castro, L. N., Hadjiosif, A. M., Hemphill, M. A. & Smith, M. A. Environmental consistency determines the rate of motor adaptation. *Curr. Biol.* **24**, 1050–1061 (2014).

67. Hadjiosif, A. M., Morehead, J. R. & Smith, M. A. A double dissociation between savings and long-term memory in motor learning. *PLoS Biol.* **21**, e3001799 (2023).

68. McDougle, S. D., Bond, K. M. & Taylor, J. A. Explicit and Implicit Processes Constitute the Fast and Slow Processes of Sensorimotor Learning. *Journal of Neuroscience* **35**, 9568–9579 (七月 1 2015).

69. Johansson, F., Hesslow, G. & Medina, J. F. Mechanisms for motor timing in the cerebellar cortex. *Curr Opin Behav Sci* **8**, 53–59 (2016).

70. Yeo, C. H., Hardiman, M. J. & Glickstein, M. Classical conditioning of the nictitating membrane response of the rabbit. I. Lesions of the cerebellar nuclei. *Exp. Brain Res.* **60**, 87–98 (1985).

71. Frey, P. W. & Ross, L. E. Rabbit eyelid conditioning: Effects of age, interstimulus interval, and intertrial interval. *Dev. Psychobiol.* **1**, 276–279 (1968).

72. Schneiderman, N. & Gormezano, I. Conditioning of the nictitating membrane of the rabbit as a function of cs-us interval. *J. Comp. Physiol. Psychol.* **57**, 188–195 (1964).

73. Smith, M. C. CS-US interval and US intensity in classical conditioning of the rabbit's nictitating membrane response. *J. Comp. Physiol. Psychol.* **66**, 679–687 (1968).

74. Op de Beeck, H. P. & Baker, C. I. The neural basis of visual object learning. *Trends Cogn. Sci.* **14**, 22–30 (2010).

75. Narain, D., Remington, E. D., Zeeuw, C. I. D. & Jazayeri, M. A cerebellar mechanism for learning prior distributions of time intervals. *Nat. Commun.* **9**, 469 (2018).

76. Wang, T. *et al.* A unitary mechanism underlies adaptation to both local and global environmental statistics in time perception. *PLoS Comput. Biol.* **19**, e1011116 (2023).

77. Vindras, P., Desmurget, M., Prablanc, C. & Viviani, P. Pointing Errors Reflect Biases in the Perception of the InitialHand Position. *J. Neurophysiol.* **79**, 3290–3294 (1998).

78. Shea, J. B. & Morgan, R. L. Contextual interference effects on the acquisition, retention, and transfer of a motor skill. *J. Exp. Psychol. Hum. Learn.* **5**, 179–187 (1979).

79. Tsay, J. S., Irving, C. & Ivry, R. B. Signatures of contextual interference in implicit sensorimotor adaptation. *bioRxiv* (2022) doi:10.1101/2022.07.03.498608.

Supplementary Information

Supplemental Result 1: State-space models fails to provide parsimonious account of learning and forgetting during adaptation.

The CPC model provides an excellent fit to the behavior observed during the perturbation and washout phases when the former involves a fixed clamp (Fig 2c). We recognize that this is not surprising given the number of parameters and relatively simple manipulation. However, this result stands in contrast to that obtained when these data are fitted with the most widely used sensorimotor adaptation model, the state-space model[44,48]. A key feature of the state-space model is that adaptation reaches an asymptote when the trial-by-trial effects of learning and forgetting cancel each other out (see Methods). While this will produce asymptotic learning, the state space model will predict a washout function that is much faster than empirically observed. The CPC model captures performance during both the acquisition and washout phases because the model includes a parameter specifying the upper boundary of adaptation, $m_{\max}$, assumed to reflect a limitation in neuroplasticity in the DCN.

To further compare the two models, we conducted a second experiment in which the post-training phase alternated between no-feedback and clamp trials (Exp 2, referred to as half-washout, Fig 2d). The state-space model predicts that the asymptote will drop to 50% because learning will only occur on 50% of the trials (feedback trials), a prediction that holds even in state-space models that posit learning at multiple time scales[18,49]. However, the asymptote showed only a slight decrease when clamped feedback was presented on 50% of the trials, consistent with the predictions of the CPC model (Fig 2d). These results highlight a major limitation in using state-space models to capture implicit adaptation even when there is no manipulation of the learning context.

Supplemental Result 2: The CPC model accounts for contextual interference.

The two-layer model provides an alternative explanation for another type of context-dependent learning, contextual interference. The term is a bit of a misnomer since the phenomenon refers to the fact that, while performance gains when training in multiple contexts is slower compared to training in a single context, retention is better in the former[78,79]. As such, exposure to multiple contexts during training actually enhances learning as measured by long-term gains. Interestingly, this phenomenon is not limited to skill acquisition tasks but is also observed in studies of implicit adaptation[78] (Fig S9).

In the revised CPC model, contextual interference occurs due to the parallel operation of labile and stable learning processes. With multiple targets (constituting multiple contexts), the rate of acquisition is slower compared to a single target since learning from the labile process decays between successive reaches to a given target. However, early retention is higher since the contribution of the labile process is small. Thus, as with anterograde interference, contextual interference arises from the dynamics of the system without postulating any representation of context.

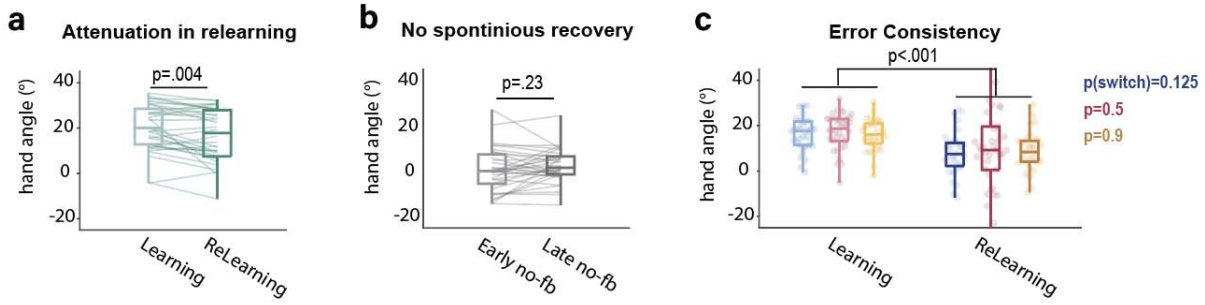

Fig. S1 Effect of experience and error consistency on implicit adaptation. a) Attenuation in relearning in Exp 4. Adaptation was attenuated in response to re-exposure to a perturbation compared to the initial exposure (t(33)=3.1, p=0.004) Data are averaged across each training phase. **b)** Spontaneous recovery was not observed in Exp 4 during the no-feedback phase after washout. Hand angle over the first 5 trials of the no-feedback phase (Early) is similar to hand angle over the last 5 trials (Late, t(33)=1.2, p=0.23). c) Error consistency did not affect adaptation during initial learning and during relearning in Exp 5. A mixed ANOVA showed a main effect of learning/relearning, (F(1,101)=37.7, p<0.001), similar to the antegrade interference observed in Exp 3. There was no effect of error consistency (F(2,101)=0.18, p=0.84) or interaction between phase and error consistency (F(2,101)=0.12, p=0.88). Box plots indicate median, max and min values, and 25% and 75% quartiles.

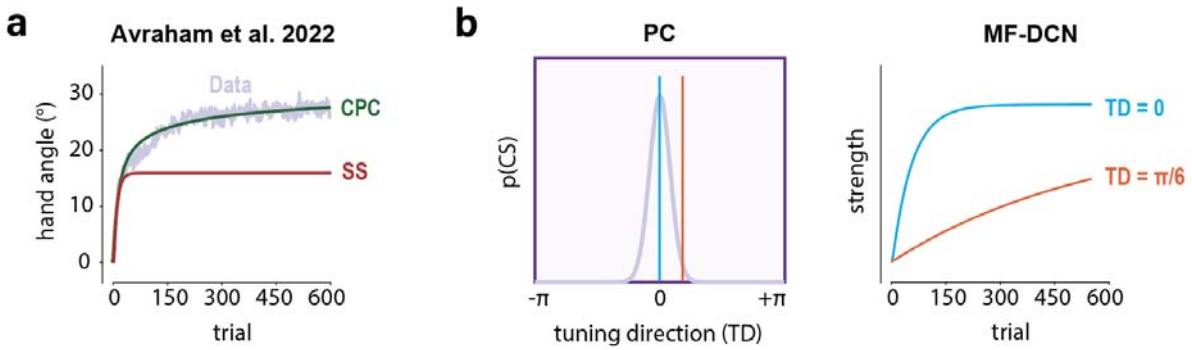

Fig. S2 The CPC model incorporates adaptation at different rates. a) Modeling adaptation learning functions frequently requires postulating multiple learning processes rather than a single-process state-space (SS) model. The panel depicts a learning curve from Avraham et al (2022) in which participants were exposed to a 30° (intermixed with 0° clamps, but not relevant for the current point). A single-process state-space model can capture the rapid change in hand angle early in learning but then saturates. However, it fails to capture the gradual increase in late adaptation. The CPC model simultaneously captures early and late adaptation through the operation of multiple learning processes. b) Cells with a tuning direction (TD) aligned to the error direction (blue) respond strongly to the error (left), driving rapid early adaptation and saturate quickly (right). Cells with tuning misaligned with the error direction (orange, π/6 in this example) have a relatively low error response early in training but make a relatively large contribution late in training. Note that "fast" and "slow" emerge from the tuning properties of units within a single layer (DCN). The net change in behavior is a composition of all activated units in the population.

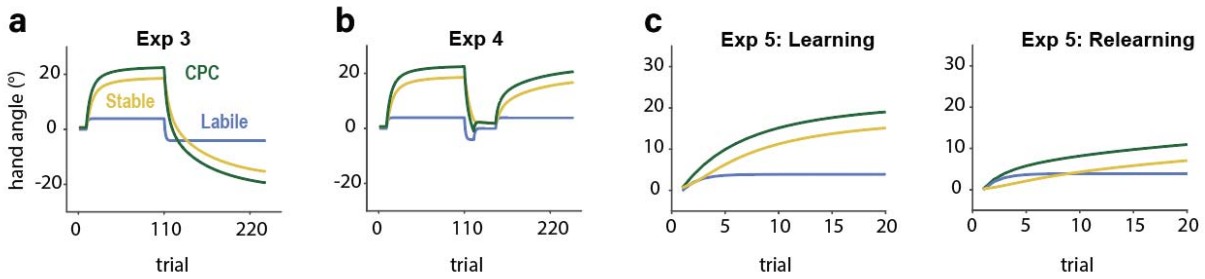

Fig. S3 Predicted time course of stable and labile processes in Exp 3-5. The stable process is responsible for anterograde interference (a) and attenuation in relearning (b-c). The labile process does not make a significant contribution to either phenomenon because of its low retention rate.

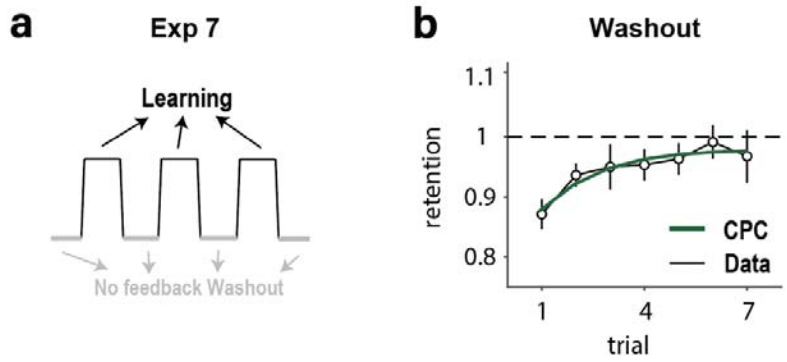

Fig. S4 Retention increases during the initial washout trials. a) To provide a stronger test of how the rate of retention changes (Exp 1), Exp 7 included mini-blocks (10 trials/mini-block) that alternated between clamp and no feedback trials. **B**) We estimated the change in retention rate over time by averaging by trial number across the no feedback blocks. Retention is relatively low in the first trials of the washout block and gradually rises ($F(6,264)=4.64$, $p<0.001$). The dark green curve shows the fit of the CPC model.

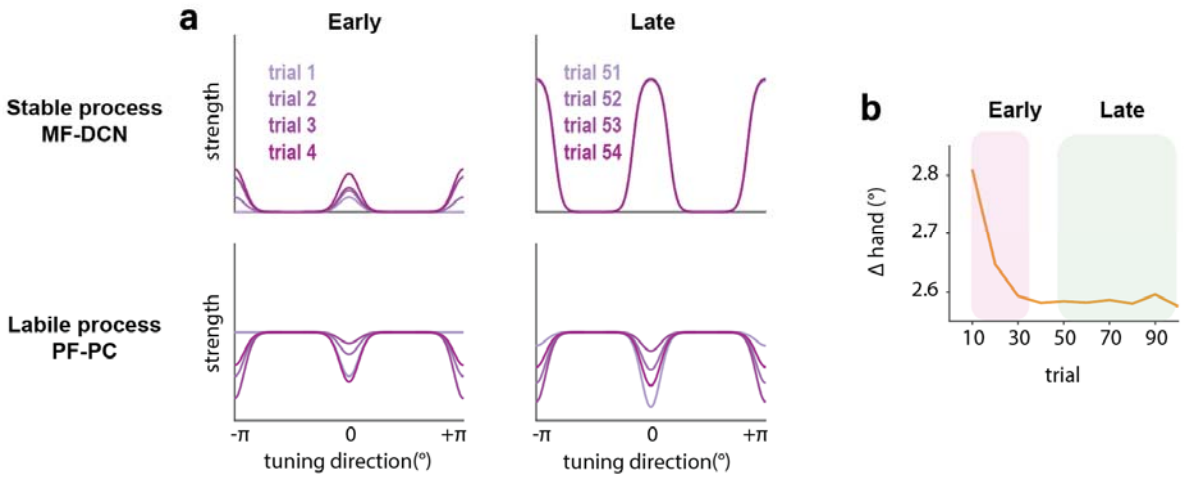

Fig. S5 Contribution of stable and labile processes in response to variable perturbations. a) The stable process (top) contributes to learning during early training and has saturated by the 50th trial. The contribution of the labile process (bottom) remains similar throughout training. **b)** Change in hand angle as a function of trial number when the size and direction of the perturbation varies across trials. The change of hand angle is larger in early training because the stable process has not saturated.

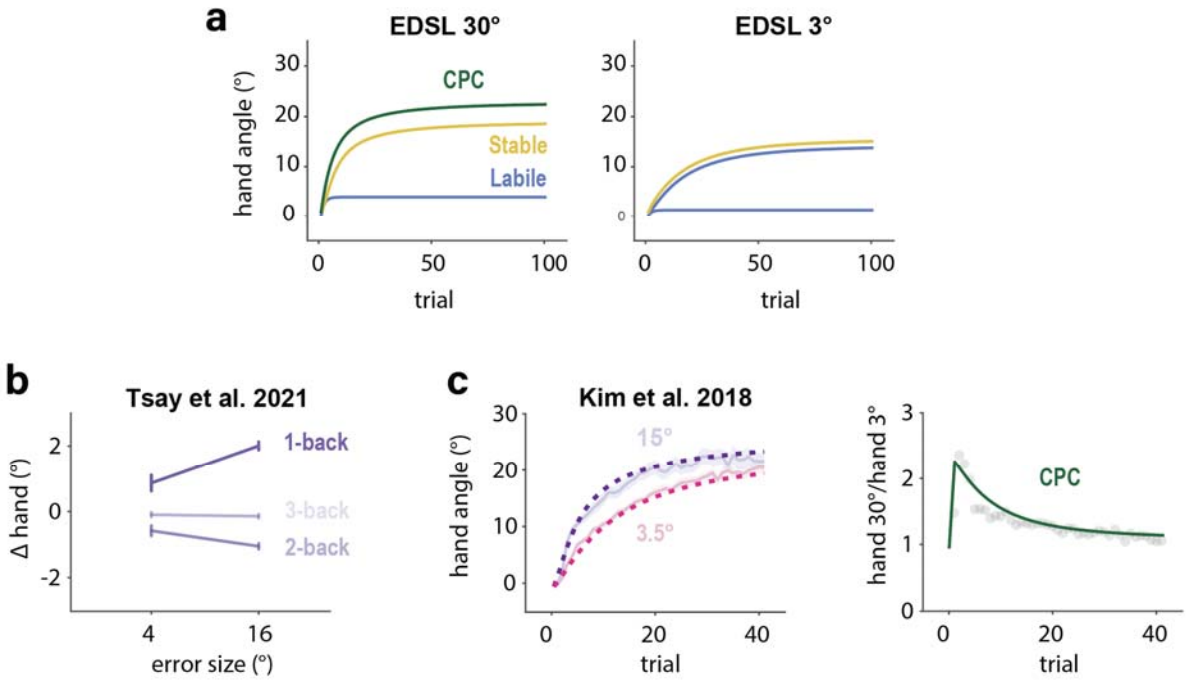

Fig. S6 Learning rates of the labile and stable processes are modulated in a similar way by error size. a) Predicted time course of state of stable and labile processes in Exp 7. Both processes are attenuated in the 3° condition compared to the 30° condition. **b)** Effect of error size on labile processes in an in-person set up, estimated from Exp 3 of Tsay et al[56] in which clamp size was 4° or 16°. **c)**, Learning functions (left) and the ratio between the two error size conditions (right) from Exp 1 of Kim et al[51] with clamp sizes of 3.5° or 15°. Dotted lines show predictions of the CPC model using the learning rate measured by Tsay et al[56]. Shaded area and error bars indicate standard error.

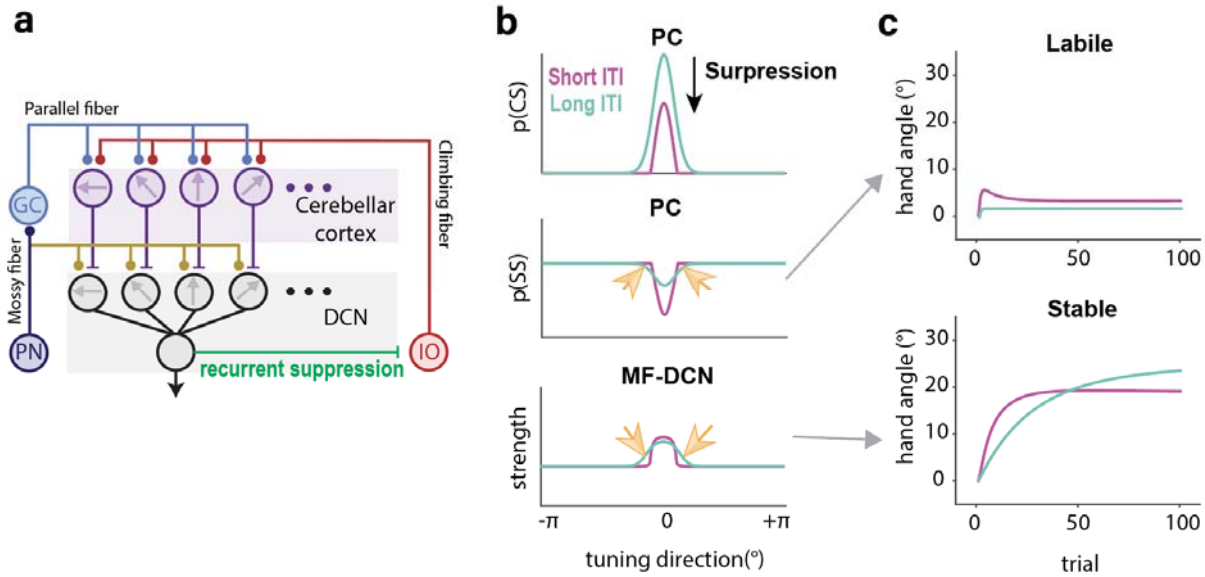

Fig. S7 Revised CPC with recurrent inhibitory pathway. The original CPC predicts that the asymptote should be lower in the long ITI condition compared to the short ITI condition because the latter includes a labile component. However, as shown in Fig 7, the asymptote is similar in the two ITI conditions. This observation motivated a revision to the CPC model in which the DCN sends a recurrent inhibitory signal to the inferior olive. **a)** Model schematic. DCN-IO inhibition suppresses the error signal to the DCN and cerebellar cortex. This suppression is generic given that the output of the DCN integrates activation across directionally tuned units. **b)** When the inter-trial-interval is short, the CS response is suppressed (top). Note that the suppression is implemented by subtracting a common value to the IO and thus alters the activation in PCs. On the next trial, SS activation is stronger in the long ITI condition since the PF-PC synapse will have recovered during the ITI (middle). However, there are a subset of tuned elements that in which SS activation is weaker in the long ITI condition (yellow arrows). This weaker activation induces adaptation in DCN units tuned to the same direction (bottom). **c)** State of the labile and stable processes over the course of a block design under long and short ITI conditions. The change in the labile process is smaller in the long ITI condition due to forgetting. The stable process is also

smaller in the long ITI condition because SS activity at the preferred error direction will dominate learning. However, the long ITI condition induces adaptation in neurons with sub-preferred error directions, resulting in larger adaptation late in training.

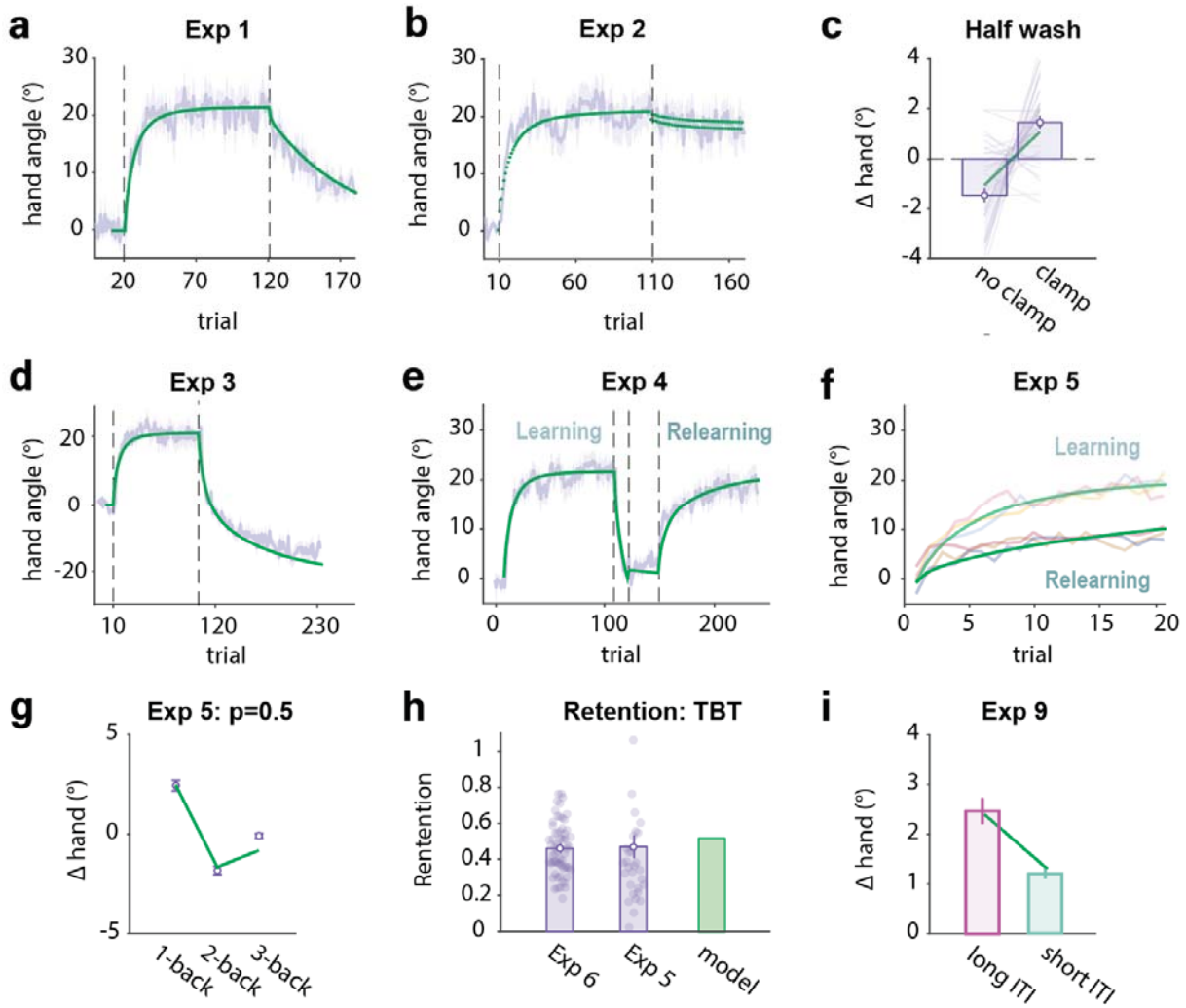

Fig. S8 Revised CPC model provides a good fit for the key results for all of the experiments. Dark green line depicts model prediction. Error bars (c, g, h, i) and shaded areas (a, b, d, e) indicate standard error.

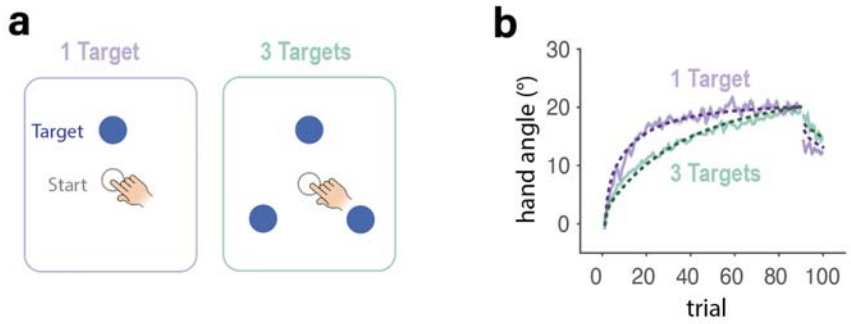

Fig. S9 Revised CPC model accounts for effect of number of target locations on adaptation. a) In Tsay et al.[79], participants were trained with either one target or three targets. In both conditions, participants reached to a single target during the washout block. **b)** Learning functions for the target location probed during washout. The 3-target condition showed slower learning but a larger aftereffect. Adding more targets is effectively akin to imposing a long ITI since successive reaches to a given target are separated by reaches to the other two locations; thus, there is more forgetting but stronger retention due to reduced contribution of labile process. Shaded area in b indicates standard error. Dash lines indicate the predictions of the Revised CPC model.

Table S1. Comparison of the CPC model and Other Models of Sensorimotor Adaptation.

	CPC	Dual State Space[18]	MoE[49]	COIN[26]	Credit Assignment[50]
Minimal attenuation in half washout (Exp 2)	✓	✗	✗	✓	✓
Anterograde interference (Exp 3)	✓	✓	✗	✓	✗
Attenuation in relearning (Exp 4)	✓	✗	✗	✗	✗
Attenuation with opposite errors but being invariant to error consistency (Exp 5)	✓	✗	✗	✗	✗
Different retention rates for trial by trial and block designs	✓	✓	✗	✓	✓
Fast single trial learning to random perturbation (Exp 6)	✓	✓	✗	✗	✓
Fast single trial learning around the asymptote (Exp 2)	✓	✗	✗	✗	✗

Comparison of models of sensorimotor adaptations on set of core phenomena. In evaluating each of the models, we used an implementation based on that presented in the associated paper (recognizing that a reasonable variant might be possible to capture more of the phenomena). The listed outcomes are described in the text with the exception of the credit assignment model (Kording et al., 2017). The credit assignment model assumes that the agent performs Bayesian inference to decompose the observed error into perturbation sources that vary across different time scales and estimates the optimal policy to compensate for them.